



UNIVERSITY OF LEEDS

This is a repository copy of *Nano-enabled bioanalytical approaches to ultrasensitive detection of low abundance single nucleotide polymorphisms*.

White Rose Research Online URL for this paper:
<http://eprints.whiterose.ac.uk/84157/>

Version: Accepted Version

Article:

Lapitan, LDS, Guo, Y and Zhou, D (2015) Nano-enabled bioanalytical approaches to ultrasensitive detection of low abundance single nucleotide polymorphisms. *The Analyst*. ISSN 0003-2654

<https://doi.org/10.1039/C4AN02304H>

Reuse

Unless indicated otherwise, fulltext items are protected by copyright with all rights reserved. The copyright exception in section 29 of the Copyright, Designs and Patents Act 1988 allows the making of a single copy solely for the purpose of non-commercial research or private study within the limits of fair dealing. The publisher or other rights-holder may allow further reproduction and re-use of this version - refer to the White Rose Research Online record for this item. Where records identify the publisher as the copyright holder, users can verify any specific terms of use on the publisher's website.

Takedown

If you consider content in White Rose Research Online to be in breach of UK law, please notify us by emailing eprints@whiterose.ac.uk including the URL of the record and the reason for the withdrawal request.



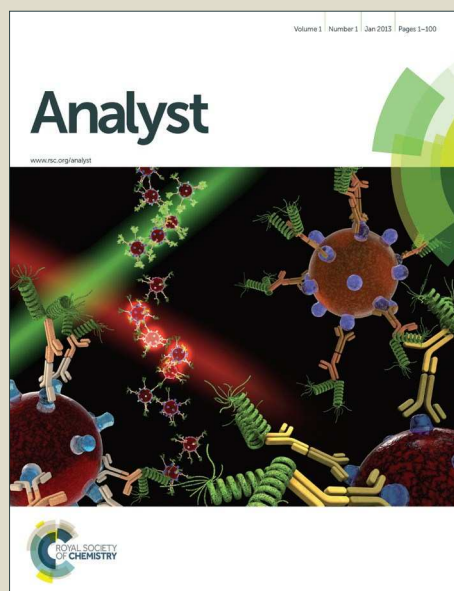
eprints@whiterose.ac.uk
<https://eprints.whiterose.ac.uk/>

Analyst

Accepted Manuscript



This article can be cited before page numbers have been issued, to do this please use: L. Lapitan, Y. guo and D. Zhou, *Analyst*, 2015, DOI: 10.1039/C4AN02304H.



This is an *Accepted Manuscript*, which has been through the Royal Society of Chemistry peer review process and has been accepted for publication.

Accepted Manuscripts are published online shortly after acceptance, before technical editing, formatting and proof reading. Using this free service, authors can make their results available to the community, in citable form, before we publish the edited article. We will replace this *Accepted Manuscript* with the edited and formatted *Advance Article* as soon as it is available.

You can find more information about *Accepted Manuscripts* in the [Information for Authors](#).

Please note that technical editing may introduce minor changes to the text and/or graphics, which may alter content. The journal's standard [Terms & Conditions](#) and the [Ethical guidelines](#) still apply. In no event shall the Royal Society of Chemistry be held responsible for any errors or omissions in this *Accepted Manuscript* or any consequences arising from the use of any information it contains.

Nano-enabled Bioanalytical Approaches to Ultrasensitive Detection of Low Abundance Single Nucleotide Polymorphisms

Lorico D.S. Lapitan Jr.,^{a,b} Yuan Guo,^a and Dejian Zhou^{a,*}

^a School of Chemistry and Astbury Centre for Structural Molecular Biology, University of Leeds, Leeds LS2 9JT, United Kingdom. Email: d.zhou@leeds.ac.uk (D.Z.).

^b Department of Chemical Engineering, Faculty of Engineering, University of Santo Tomas, Espana Boulevard, Manila, Philippines.

Abstract

Single nucleotide polymorphisms (SNPs) constitute the most common types of genetic variations in the human genome. A number of SNPs have been linked to the development of life threatening diseases including cancer, cardiovascular diseases and neurodegenerative diseases. The ability for ultrasensitive and accurate detection of low abundant disease-related SNPs in bodily fluids (*e.g.* blood, serum, etc.) holds a significant value in the development of non-invasive future biodiagnostic tools. Over the past two decades, nanomaterials have been utilized in a myriad of biosensing applications due to their ability of detecting extremely low quantities of biologically important biomarkers with high sensitivity and accuracy. Of

1
2
3
4 particular interest is the application of such technologies in the detection of SNPs. The use of
5
6 various nanomaterials, coupled with different powerful signal amplification strategies, has
7
8 paved the way for a new generation of ultrasensitive SNP biodiagnostic assays. Over the past
9
10
11
12
13
14
15
16
17
18
19
20
21
22
23
24
25
26
27
28
29
30
31
32
33
34
35
36
37
38
39
40
41
42
43
44
45
46
47
48
49
50
51
52
53
54
55
56
57
58
59
60

particular interest is the application of such technologies in the detection of SNPs. The use of various nanomaterials, coupled with different powerful signal amplification strategies, has paved the way for a new generation of ultrasensitive SNP biodiagnostic assays. Over the past few years, several ultrasensitive SNP biosensors capable of detecting specific targets down to the ultra-low regimes (*ca.* aM and below) and therefore holding great promises for early clinical diagnosis of diseases have been developed. This mini review will highlight some of the most recent, significant advances in nanomaterial-based ultrasensitive SNP sensing technologies capable of detecting specific targets on the attomolar (10^{-18} M) regime or below. In particular, the design of novel, powerful signal amplification strategies that hold the key to the ultrasensitivity is highlighted.

1. Introduction

The completion of the human genome project in 2003 [1] has led to several important discoveries relating to structure of the human genome: it is characterized by variations in DNA nucleotide sequences of one or more bases in genes of the same population [2-3]. These variations in DNA impart certain phenotypic traits that distinguish an organism from another. If such variations occur in greater than one percent of the human population, they are collectively referred to as polymorphisms. On the other hand, variations occurring in less than one percent of the population are often termed as “mutations” which are associated with

1
2
3
4 a detrimental phenotype such as those linked with various cases of cancer [3]. The most
5
6
7 common sequence variation occurring in the human genome is the stable substitution of a
8
9
10 single nucleotide, also known as single nucleotide polymorphisms (SNPs). The human
11
12
13 genome has been estimated to contain more than 10 million SNPs which are distributed
14
15
16 across the human genome at an estimated frequency of at least one nucleotide every 1000
17
18
19 base pairs but with apparent regional differences [4-5]. While most SNPs do not alter the
20
21
22 metabolic function and expression levels of a gene, some do result in differences in
23
24
25 predisposition to certain heritable diseases [6-8], response to drugs (pharmacogenetics) [9-
26
27
28 10], and perception of pain [11]. Several studies have shown that SNPs are closely associated
29
30
31 with many types of cancer and presupposes the risk of cancer progression [12-15]. For
32
33
34 instance, it was observed that single point mutations in the KRAS gene at codons 12, 13, and
35
36
37 61 are associated with the development of certain pancreatic [14] and lung cancers [15].
38
39
40 Moreover, numerous detrimental and inheritable diseases such as diabetes [7], vascular
41
42
43 diseases [16], some forms of neurodegenerative and mental illness [17-18] have also been
44
45
46 linked to SNPs. On the other hand, microRNAs (miRNAs) which are 17 – 24 base short RNA
47
48
49 molecules playing important roles in numerous cellular processes such as differentiation,
50
51
52 cellular growth, and apoptosis. Point mutations in miRNAs have been associated with several
53
54
55 forms of cancers, affecting the cancer risk and treatment efficacy in some non-small cell lung
56
57
58 cancer patients [19-20]. These are just a few examples highlighting the association of SNPs in
59
60

1
2
3
4 relation to human diseases and treatment responses, demonstrating the tremendous value of
5
6
7 SNPs in biomedical research. Indeed, SNPs are considered as an important class of
8
9
10 biomarkers that could allow scientists and medical practitioners to better understand certain
11
12
13 diseases, develop novel non-invasive diagnostics tool and ultimately allow for a more
14
15
16 personalized approach to disease treatment and therapies.

17
18 The most established techniques for point mutation detections in DNA have largely
19
20
21 relied on the amplification power of the polymerase chain reaction (PCR) coupled with
22
23
24 quantitative fluorescence detection and/or DNA sequencing techniques such as pyro-/next
25
26
27 generation sequencing of the amplified product. Although highly sensitive and widely used,
28
29
30 such methods can sometimes introduce errors during the PCR exponential amplification
31
32
33 process which is sensitive to contaminations and hence may affect diagnostic accuracy [21-
34
35
36 22]. PCR is also often regarded as labor-intensive and time-consuming, making it unsuitable
37
38
39 for rapid, point-of-care diagnostics. Moreover, it also requires an expensive thermal cycler
40
41
42 and thereby the cost per analysis might be high for developing countries. These limitations
43
44
45 have largely hampered the wide use of PCR for rapid, on-site diagnostics. In the case of point
46
47
48 mutation detections involving miRNAs, the real-time quantitative reverse transcription
49
50
51 polymerase chain reaction (qRT-PCR) is often the method of choice due to its high
52
53
54 sensitivity. However, several drawbacks do exist for the qRT-PCR, including complex
55
56
57 processes such as reverse transcription, multiple primer design, and precise temperature
58
59
60

1
2
3
4 control [23]. Unsurprisingly, many of the recent developments have focused on developing
5
6 PCR-free alternatives in SNP biosensing. The reliable detection of low abundance specific
7
8 SNPs without PCR pre-amplification represents an extremely challenging albeit exciting
9
10 research area of the bioanalytical science.
11
12

13
14
15
16
17
18
19
20
21
22
23
24
25
26
27
28
29
30
31
32
33
34
35
36
37
38
39
40
41
42
43
44
45
46
47
48
49
50
51
52
53
54
55
56
57
58
59
60

Over the past few years, enormous efforts have been directed towards the development of novel, ultrasensitive PCR-free SNP assays and a number of techniques have been developed [22, 24-27]. The detection and quantification of known SNPs are primarily based on the specificity of target hybridization [28-29] and enzyme discriminations, such as specific enzymatic cleavage [30], and single base primer extension [31-32]. Of particular interest in the early stages of PCR-free SNP biosensing development has been based on using water-soluble, cationic conjugated polymers (CCPs) as fluorescence transducers. For example, the Leclerc group [33-34] has pioneered and developed DNA detection based on the electrostatic attraction between a cationic polythiophene and DNA. The colour and fluorescence changes of the polymer in the presence of single-stranded and double-stranded DNAs were used as the basis for biosensing. They have reported the first detection of SNPs directly from clinical samples without the need of DNA pre-amplification with an impressive detection limit of 3 zeptomolar. The Bazan and Hageer groups have also detected specific DNA sequences *via* CCP sensitised Förster resonance energy transfer (FRET) to dye-labelled probes [35-36]. The electrostatic attraction between the cationic CCPs and the anionic DNAs leads to short

1
2
3
4 distance donor (CCP)-acceptor (DNA dye-label), hence strong FRET [37]. A substantive
5
6
7 review of such work has already been provided by Swager *et al.* [38], and hence this will not
8
9
10 be main topic here.

11
12
13 Recently, the use of various nanomaterials has provided the capability of ultrasensitivity
14
15 and high specificity in SNP detection. Nanomaterials have been well-studied primarily
16
17 because of their unique, size dependent physical and chemical properties. In terms of
18
19 biosensing applications, such useful properties include extremely large surface area, tunable
20
21 surface chemical composition that allow easy and controlled immobilization of stable
22
23 bioreceptors for efficient transduction of target binding into strong readout signals. These
24
25 properties are advantageous for achieving ultrasensitivities, allowing easy integration into
26
27 miniaturized devices ushering an era of next generation cost-effective SNP diagnostics.

28
29 Nanomaterials such as metallic nanoparticles (NPs) [39-44,55], quantum dots (QDs) [45-48],
30
31 magnetic nanoparticles (MNPs) [49-54], and carbon based nanomaterials [56] have been
32
33 combined with biomolecules such as enzymes, oligonucleotides and DNazymes to develop
34
35 sensors for detection and quantification of cancer-specific SNPs. Such nanomaterial-based
36
37 SNP assays have been coupled with a number of different readout strategies, including
38
39 colorimetry, fluorimetry, surface enhanced Raman spectroscopy (SERS), electrochemical and
40
41 electrochemiluminescence *etc.* For example, Boudreau and colleagues recently reported the
42
43 use of FRET-based CCP transducers by combining them with highly fluorescent core - shell
44
45
46
47
48
49
50
51
52
53
54
55
56
57
58
59
60

1
2
3
4 nanoparticles. The Ag nanoparticle core was used to amplify the optical signal generated
5
6 upon target recognition. This plasmonic enhancement resulted to the direct detection of
7
8 unamplified target nucleic acid at femtomolar concentration regime [57-59].
9
10

11
12 Table 1 summarizes some of the recently developed ultrasensitive SNP assays using
13
14 different nanomaterials coupled with different probe and/or signal amplification strategies.
15
16 The sensitivities and specificities of these assays are already comparable to, or even surpass
17
18 those of many PCR based techniques, demonstrating the high suitability of nanomaterials for
19
20 ultrasensitive SNP detection. Despite significant developments, it is important to consider
21
22 some other burgeoning challenges in clinical diagnosis, particularly in the quantification of
23
24 extremely low abundant SNPs in an overwhelming background of wild-type genes in clinical
25
26 settings. Moreover, the ability of simultaneous detection of multiple targets is also important
27
28 for high diagnostic accuracy because *“no tumor marker identified to date is sufficiently*
29
30 *sensitive or specific to be used on its own to screen for cancer”* [60-61]. The practical
31
32 importance of these relies on the fact that most cancer cases are only diagnosed in the late
33
34 stage and when the chances of patient survival are already slim. As a result, early diagnosis is
35
36 of paramount importance for improving the survival and prognosis of cancer patients. All
37
38 these necessitate the development of ultrasensitive assays with multiplexing capability that
39
40 can detect the extremely low concentrations of cancer-specific SNPs in clinically media.
41
42
43
44
45
46
47
48
49
50
51
52
53
54

55
56 In general, three different approaches are widely employed to improve the assay
57
58
59
60

1
2
3
4
5
6
7
8
9
10
11
12
13
14
15
16
17
18
19
20
21
22
23
24
25
26
27
28
29
30
31
32
33
34
35
36
37
38
39
40
41
42
43
44
45
46
47
48
49
50
51
52
53
54
55
56
57
58
59
60

detection limits: target, probe, and signal amplification. Among these, target amplification is mainly achieved *via* enzyme-mediated replication of target nucleic acid sequences, leading to *ca.* 10^8 - 10^9 fold amplification of target concentration to make it high enough to be readily detected by traditional approaches such as gel electrophoresis [22]. An excellent example here is the well established polymerase chain reaction (PCR). More recently, isothermal target amplification strategies have also been developed [24-27, 62] and displayed sensitivities comparable to that of the PCR. In contrast, probe amplification does not change the copy number of the target, but instead the probe sequence which is complementary to the target is amplified and detected by conventional hybridization method. Signal amplification strategies are approaches that amplify the analytical signal generated by each labeled or unlabelled probe so as to increase the assay sensitivity. Various signal amplification strategies have been used to increase the sensitivity of the probe-based assays.

In this mini-review, we will highlight some of the most recent advance in the field of nanomaterial-based SNP detection, with a particular focus on those techniques capable of detecting and quantifying extremely low target concentrations down to the attomolar regimes or below. Given the high specificity, the hybridization-based method remains one of the most popular methods for nanomaterial based SNP assays. In general, the ultra-sensitivity of these assays have been achieved through one of the following five different strategies, [i] nanoparticle–target assisted PCR amplification, [ii] nanoparticle-target assisted probe

1
2
3
4 amplification, [iii] target recycling coupled with probe amplification, [iv] tandem
5
6
7 amplification coupled with signal catalytic cascades, and [v] nanomaterial enhanced signal
8
9
10 amplification. Each of these classes will be discussed in this review with a focus on the assay
11
12 sensitivity and comment on their applicability to real biological matrices. Moreover, a critical
13
14 categorization of such existing approaches on the basis of different amplification strategies is
15
16
17
18
19 proposed.

(i) Nanoparticle – Target Assisted PCR Amplification Strategy

20
21
22
23
24
25
26
27
28
29
30
31
32
33
34
35
36
37
38
39
40
41
42
43
44
45
46
47
48
49
50
51
52
53
54
55
56
57
58
59
60
An essential first step in this approach is to pre-amplify the extremely low abundant
SNP target into sufficiently high number of copies so that it can be readily detected by
conventional methods. Given its extremely powerful exponential amplification power, it is
unsurprising that PCR-based SNP biosensing assays have been reported to have high
sensitivities.^[63] In particular, the incorporation of plasmonic nanomaterials such as Au and
Ag nanoparticles has been recently combined with PCR pre-amplification of the target DNA,
leading to unprecedented sensitivities. For example, Kotov and colleagues have reported an
unexpected chirality of bridged metallic nanoparticle dimers and have exploited this in
ultrasensitive biosensing. They have prepared different sized Au and Ag NPs and
functionalized them with specific antibodies so that they can sandwich bind the specific target
protein (*e.g.* prostate specific antigen PSA, a cancer marker) and assemble into hetero-

1
2
3
4 nanoparticle dimers. These biomolecule bridged NP heterodimers are chiral, leading to an
5
6 observable change in circular dichroism (CD) spectra over 350-600 nm region. The authors
7
8 found that this assay was extremely sensitive, capable to detecting PSA down to the sub-aM
9
10 level with an extremely impressive detection limit (DL) of 1.5×10^{-20} M and a linear dynamic
11
12 range of ~ 3 orders of magnitude. Such a highly impressive sensitivity has been attributed to
13
14 plamonic enhancement of intrinsic chirality of biomolecules, strong optical coupling of
15
16 photons with twisted NP heterodimers, and bisignate nature of the CD spectra [64-65].

17
18 This assay has been recently modified to suit the detection of ultralow concentrations of
19
20 DNA [66] by applying a PCR amplification of the dsDNA with primers linked to Au NPs (25
21
22 nm Au NP-linked forward primer and 10 nm Au NP-linked reverse primer) in the presence of
23
24 Taq polymerase and dNTPs (see Fig. 1). The DNA-bridged Au NP heterodimers displayed
25
26 circular dichromism (CD) bands at 260 and 525 nm, attributed to the chiral secondary
27
28 structures of duplex DNA and the chiral NP dimers, respectively. These dimers displayed
29
30 unexpected chirality due to the ellipsoidal shape of the NPs and a scissor-like configuration
31
32 with two long NP axes forming a dihedral angle of 10° . Coating of the Au NP dimers with Ag
33
34 or Au are found to affect their chiro-plasmonic activity: as the thickness of the Ag shell
35
36 increased, the intensity of the CD bands also increased and shifted from 525 to 418 nm. In the
37
38 case of Au coating, increasing the Au shell thickness resulted in a color change of the
39
40 dispersion from pink to purple and the CD bands exhibited a 61 nm red shift. More
41
42
43
44
45
46
47
48
49
50
51
52
53
54
55
56
57
58
59
60

1
2
3
4 importantly, Au coating of DNA-bridged Au NP dimers gave fairly narrow spectra with high
5
6 optical anisotropy. Optimization of assay parameters such as specific design of primers and
7
8 number of PCR cycles has yielded ultrasensitive DNA assay with a linear dynamic range
9
10 spanning 7 orders of magnitude (from 160 zM to 1.6 pM) and an extremely low DL of 17
11
12 zM. Currently, this method reported the highest sensitivity for DNA detection using
13
14 nanomaterials based sensing platforms, and hence appears to have good potential for genetic
15
16 based early diagnostic applications. Despite such great sensitivity, the applicability of this
17
18 assay towards the detection and discrimination of specific SNP's in complex media such as
19
20 the wild-type DNA background has yet to be demonstrated. Moreover, given the fact that this
21
22 assay requires PCR pre-amplification, it is less well-suited to applications that require rapid
23
24 results such as the point-of-care diagnostics.
25
26
27
28
29
30
31
32
33
34
35
36
37
38

39 (ii) Nanoparticle - Target Assisted Probe Amplification Strategy

40
41 Rolling circle amplification (RCA) [67-69] and ligase chain reaction (LCR) [70-72] are two
42
43 of the most extensively used probe amplification strategies in SNP detections. Recently,
44
45 nanomaterials have been combined with these probe amplification assays, leading to further
46
47 improvements in detection limits. These assays typically use a complementary
48
49 oligonucleotide capture probe chemically linked to an Au nanoparticle, quantum dot, or
50
51 magnetic nanoparticle to directly interact with their specific analytes, thereby amplifying
52
53
54
55
56
57
58
59
60

1
2
3
4 molecular recognition events such as DNA hybridization. In addition, magnetic nanoparticles
5
6
7 have been further used for target capture, enrichment and purification which can further
8
9
10 enhance the assay sensitivity.

11
12 Unlike PCR which requires thermal cycles, RCA is an isothermal probe amplification
13
14 strategy using a single-stranded DNA as a padlock probe (Fig. 2A). The 5'- (phosphate
15
16 modified) and 3'- terminal fragments of the padlock probe are specifically designed to be
17
18
19 complementary to the target DNA. Hybridisation of the target to the padlock probe then
20
21
22 brings its 5'- and 3'- terminus close to each other, forming a nicked circle which can be
23
24
25 covalently ligated together by a DNA ligase if the padlock and target sequences are fully-
26
27
28 matched, forming a circularized padlock probe. The circularised padlock probe is then
29
30
31 amplified by a ϕ 29 polymerase in the presence of dNTP's, producing a greatly elongated
32
33
34 single-stranded DNA containing numerous copies of repeat tandem sequence units
35
36
37 complementary to the circular padlock probe. In contrast, the presence of a single-base
38
39
40 mismatch at the nicked target/padlock duplex probe can prevent the specific ligation and
41
42
43 formation of the circular padlock probe, and therefore no RCA amplification (Fig. 2B). The
44
45
46 stringent requirement of full sequence complementary between the padlock and target to form
47
48
49 the ligated circular padlock probe allows the RCA strategy to have excellent specificity for
50
51
52 SNP detection [42, 77].
53
54

55
56 Similar to PCR, the ligase chain reaction (LCR) also requires multiple thermal cycles to
57
58
59
60

1
2
3
4 achieve specific ligation of two short DNA probes catalysed by a DNA ligase into a single
5
6 strand templated by a full-match DNA target [24-27]. In a typical SNP assay, LCR uses two
7
8 pairs of probes each containing two short complementary oligonucleotides, but the overall
9
10 sequence is complementary to the target DNA sequence (Fig. 3). After thermal denaturation
11
12 followed by annealing, a pair of the probes are hybridized to one of the denatured target DNA
13
14 strand. They are subsequently ligated by a DNA ligase if the probes and target sequences are
15
16 fully complementary at the nick site. On the other hand, the presence of single-base mismatch
17
18 at the nick site can prevent specific ligation, allowing for the LCR to have high SNP
19
20 selectivity. After the first ligation round, each ligated product can then function as a new
21
22 template to ligate further probes in the following thermal cycles. Repeating the thermal cycles
23
24 thus leads to an exponential increase of the ligated probes. Ligation reactions have better
25
26 single-base mismatch discriminatory ability than primer extension methods, making LCR
27
28 more specific for SNP detection than PCR based methods [24].
29
30
31
32
33
34
35
36
37
38
39
40
41

42 A particularly attractive SNP assay has been the colorimetric sensing using Au NPs
43
44 because of their extremely strong surface plasmon resonance (SPR) absorption at ~520 nm
45
46 ($\epsilon > 10^9 \text{ M}^{-1} \cdot \text{cm}^{-1}$ for a 20 nm Au NP, 4-5 orders of magnitudes stronger than typical organic
47
48 dyes), making it strongly colored even at low nM concentrations. Moreover, its SPR band is
49
50 also sensitive to aggregation, isolated Au NPs appear red but aggregated ones are blue or
51
52 purple. The resulting color change is distinct and clearly visible by the naked eye [27]. Here
53
54
55
56
57
58
59
60

1
2
3
4 specific DNA targets that can induce the aggregation of Au NPs have been used to detect
5
6
7 SNPs, taking the full advantage of the very sharp melting transition for the sandwich duplex
8
9
10 formed between the target DNA and a pair of probe DNA (with sequence complementary to
11
12
13 each half of the DNA target) modified Au NPs. The sharp melting transition means a single-
14
15
16 base mismatch between the target and probes can be distinguished due to their slightly
17
18
19 different thermal stability. This leads to distinct color changes at elevated temperatures that
20
21
22 can be exploited for SNP detection [73-74]. Combined with various amplification strategies,
23
24
25 such assays have achieved pretty low detection limits, down to the femtomolar region.

26
27 More recently, LCR has been combined with Au NP for ultrasensitive colorimetric SNP
28
29
30 detection by the Gao group [40]. The assay involves the real time ligation of oligonucleotide
31
32
33 coated Au NPs templated by the complementary SNP target (Fig. 4A). In each LCR cycle,
34
35
36 there is an increasing amount of Au NPs being ligated that are subsequently used to template
37
38
39 the ligation of further Au NPs, leading to an exponential increase in the amount of
40
41
42 covalently linked Au NPs. Since the SPR band of Au NPs is sensitive to NP assembly, this
43
44
45 resulted in a color change that can be directly monitored by UV-vis (Fig. 4B). This assay has
46
47
48 an impressive linear dynamic range of 6 orders of magnitude and is capable of detecting
49
50
51 specific DNA targets down to 20 aM. This assay also has high selectivity: it can specifically
52
53
54 detect the wild-type (WT) KRAS gene in the presence of large excesses of genomic DNAs
55
56
57 even at 1:100000 (KRAS:genomic DNA) base pair ratios when readings were taken at 90
58
59
60

1
2
3
4 °C. At this temperature, all non-chemically ligated DNA–Au NP conjugates were dislodged,
5
6 leaving only the covalently ligated Au NPs in the solution. Thus, the incorporation of
7
8 ligation allowed for easy elimination of interferences from coexisting DNA and a reduced
9
10 background. This assay has been further detected the WT-KRAS in the presence of KRAS
11
12 single point mutants, yielding an impressive SNP selectivity factor of 2000. This assay can
13
14 be used as an efficient approach for detecting specific mutant DNAs by simply redesigning
15
16 the sequences of capture probes and signal probes, and thus has great potential for
17
18 ultrasensitive detection of various disease-related SNPs. Despite such great promises, the
19
20 relatively long assay time and requirement of multiple thermal cycles may limit its use in
21
22 rapid, point-of-care applications.
23
24
25
26
27
28
29
30
31
32

33 Although the LCR strategy appears to be a highly attractive alternative to PCR
34
35 amplification, an apparent weakness has been its low amplification efficiency when being
36
37 combined with nanomaterials. This is due to the restricted accessibility of the ligases to the
38
39 ligation site in oligonucleotide modified Au NPs. In an attempt to overcome the limitations of
40
41 conventional LCR, a process called enzyme-free click chemical ligation reaction (CCLR) that
42
43 involves Au NP and magnetic bead was developed by Kato and colleagues [75] (Fig. 5A).
44
45 Unlike the earlier cross-linked Au NP systems, this assay does not require the use of ligases
46
47 to carry out LCR and does not require the formation of large assemblies. The CCLR method
48
49 uses an azide-containing DNA modified Au NP and a dibenzocyclooctyne-containing biotin-
50
51
52
53
54
55
56
57
58
59
60

1
2
3
4 DNA probe. Sandwich hybridization of the target DNA (RNA) with the azide-DNA modified
5
6 Au NP and biotin-DNA lead to enzyme-free ligation *via* the copper-free click chemistry,
7
8 producing biotin–ligated Au NPs. Repeating the thermal cycles lead to the biotin-ligated Au
9
10 NPs being exponentially amplified, which are then captured by using streptavidin–modified
11
12 magnetic beads. After magnetic separation, the strong absorption of the Au NP can be used to
13
14 detect and quantify the target DNA (RNA). Using this assay strategy, a DNA sequence
15
16 associated with the hepatitis A virus Vall 7 polyprotein gene (HAV) has been detected at a
17
18 concentration as low as 50 zM with a linear dynamic range of 3 orders of magnitude (Fig. 5
19
20 B), which is highly impressive. However, it should be noted that the absolute signal
21
22 difference throughout the whole dynamic range was relatively small, being only ~30% (*e.g.*
23
24 increased from ~1.0 to 1.3), which can significantly limit its diagnosis accuracy. This method
25
26 can also discriminate specific single point mutations, with the G-, T-, and C- Mutant signals
27
28 being 17, 0, and 0% of that of the full-match control respectively. This shows that this assay
29
30 has an excellent SNP discrimination, although a more useful demonstration of the SNP
31
32 specificity would be the ability to detect low specific target SNPs in a background of wide-
33
34 type genes under clinical relevant media [75].
35
36
37
38
39
40
41
42
43
44
45
46
47
48
49
50
51
52

53 (iii) Target recycling coupled with probe and/or signal amplification.

54
55
56 Target recycling is another useful strategy to amplify low copy number SNPs. In this
57
58
59
60

1
2
3
4 strategy, the target DNA is cycled in a number of hybridization events, each time producing
5
6 one or several copies of the complementary probe strand, depending on the approaches used.
7
8
9
10 However, the linear amplification nature of target recycling process has largely limited its
11
12 detection limit to the fM regime only [53,76].
13

14
15 More recently, target recycling has been combined with several other probe
16
17 amplification strategies to further improve detection limits. A significantly higher sensitivity
18
19 has been achieved by Ju and colleagues [46] who have designed a *template enhanced*
20
21 *hybridization process or TEHP* coupled with rolling cycle amplification. This target recycling
22
23 hybridization assay uses a biotinylated molecular beacon [MB] bound to a streptavidin coated
24
25 plate as the template. Hybridization of the target DNA and an assistant DNA to the loop
26
27 region of the MB forms a “Y” shaped junction (Fig. 6A). This configuration provided a
28
29 specific nucleotide sequence that can be nicked by a suitable endonuclease. Once released,
30
31 the target DNA and assistant DNA initiate another round of hybridization and strand scission
32
33 cycle. The numerous MB fragments left in the plate then served as primers for the RCA
34
35 process to produce thousands of repeat oligonucleotide sequences. These repeated sequences
36
37 then are hybridized to an oligonucleotide functionalized CdTe QD and separated. The QDs
38
39 are then dissolved by an acid, releasing greatly amplified Cd²⁺ ions that are detected by
40
41 square wave voltammetry. The combination of TEHP and RCA coupled with the use of QD
42
43 based signal tags has offered an enormous amplification of the DNA target, allowing for
44
45
46
47
48
49
50
51
52
53
54
55
56
57
58
59
60

1
2
3
4 greatly increased assay sensitivity. An impressive sensitivity of 11 aM has been attained
5
6 together with a wide dynamic range of 6 orders of magnitude (Fig. 6 B-C). This assay was
7
8 also able to discriminate the perfect complementary DNA target against various mismatch
9
10 targets with a discrimination ratio of 3.8, 5.7 and 6.6 fold for the single-base, three-base
11
12 mismatch and non-complementary oligonucleotides, respectively. Despite a high sensitivity,
13
14 the mutant discrimination ratio here is relatively moderate compared to other specific SNP
15
16 assays, which may limit its potential for applications in real clinical samples where the
17
18 presence of large background genomic DNAs and/or wild-type genes may strongly interfere
19
20 the specific SNP detection.
21
22
23
24
25
26
27
28
29
30
31
32

33 (iv) Tandem amplification schemes and signal catalytic cascades

34
35 In order to achieve detections in even lower concentration regimes, several researchers
36
37 have reported the use of tandem amplification schemes [42, 77-78]. The combination of two
38
39 amplification strategies has been deemed necessary to further improve the sensitivity and
40
41 specificity of SNP detection. Moreover, this strategy can overcome the low amplification
42
43 efficiency by a single amplification scheme.
44
45
46
47
48
49

50 The colorimetric detection of SNPs using a combination of RCA and nicking
51
52 endonuclease-assisted nanoparticle amplification strategy was developed by Xu and
53
54 colleagues [42]. In this assay, ligation was performed when the target DNA was hybridized
55
56
57
58
59
60

1
2
3
4 with the padlock probe, leading to a circularized template. Subsequent RCA reaction in the
5
6 presence of dNTPs led to the formation of a long single strand DNA. Nicking reactions at
7
8 many of the repeated sites along the RCA elongated single-stranded DNA occurred
9
10 simultaneously. Upon completion of the strand scission cycles, the addition of a specific
11
12 oligonucleotide modified Au NP provided a simple, colorimetric detection of target DNA
13
14 down to 1 pM.
15
16
17
18
19
20

21 The sensitivity of ligation assays can be further improved when being coupled to another
22
23 probe amplification scheme. For example, the combination of LCR and RCA in detecting
24
25 SNPs has been recently demonstrated by Cheng and colleagues, [77] who has demonstrated
26
27 the sensitive detection of 1 fM of unlabeled target DNA under the optimised assay conditions.
28
29
30
31
32

33 Further improvements of assay sensitivity have been achieved by incorporation of
34
35 DNAzymes (catalytic nucleic acids) based catalytic cascades signal amplification. In this
36
37 regard, Zhang and colleagues [50] have designed a new RCA amplification approach where
38
39 the presence of the target KRAS SNP triggers the ligation of the padlock probe.
40
41 Subsequently, multiple other circular templates were interlocked to the padlock probe by
42
43 means of complementary sequence forming an ABABAB-type DNA copolymer (Fig. 7A).
44
45 The inter- locked circular primers containing the HRP-mimicking DNAzymes subsequently
46
47 underwent another round of RCA, producing long, single-strand DNA products each
48
49 containing thousands of copies of the repeated DNAzyme sequences acting catalytic units.
50
51
52
53
54
55
56
57
58
59
60

1
2
3
4 The incorporation of numerous such catalytic units thereby greatly enhanced the
5
6 chemiluminescence signal in the presence of luminol and H₂O₂, leading to an impressive
7
8 detection limit of 71 aM for the target SNP. This assay also provided excellent performance
9
10 in quantitative analysis in human blood serum with a linear dynamic range of 2 orders of
11
12 magnitude with good signal linearity from 0.1-10 fM (Fig. 7 B-C). The excellent sensitivity
13
14 of this assay lies on the inherent capacity to generate great amplification as a consequence of
15
16 the high turnover reaction of DNAzymes. This assay was also highly specific, and can detect
17
18 1 fM specific mutant target in the presence of 10 pM wild-type gene background. It
19
20 demonstrated a SNP detection capability of 1 in 10 000 (SNP versus wild-type target) level,
21
22 which is among the best reported in literature. Hence, combining high sensitivity and
23
24 specificity, this assay appears to have excellent potential for SNP based disease diagnostics
25
26 by specific detection of the low abundant mutated target in clinical laboratory settings. This
27
28 assay, however, is relatively complex and requires multiple amplification cycles, making it
29
30 less well-suited for rapid, point-of-care applications.
31
32
33
34
35
36
37
38
39
40
41
42
43

44 Recently, the Zhang group has developed an ultrasensitive miRNA assay based on
45
46 primer generation - mediated rolling circle amplification [PG-RCA]. This assay was used to
47
48 analyze the point mutation of mir-196a2 [T →C] in the lung tissue samples of non small cell
49
50 lung cancer patients [78]. In this assay, the presence of target mir-196a2T circularizes the
51
52 padlock probe and the mir-196a2T further functioned as a primer to initiate the next round of
53
54
55
56
57
58
59
60

1
2
3
4 RCA reaction in the presence of Vent (exo-) polymerase. This resulted in a long single-
5
6 stranded RCA product containing numerous restriction sites for *Nb.BsmI*. The RCA product
7
8 was then nicked by *Nb.BsmI*, generating a large number of new primers that was further used
9
10 to initiate a new RCA reaction. The amplified DNA products were subsequently hybridized
11
12 with a biotin/Cy5-labeled capture probes to form a double-stranded DNA. This DNA duplex
13
14 contains a recognition site for the *Nt.BstNBI* nicking enzyme, and after the nicking reaction
15
16 the capture probe was cleaved, separating Cy5 and biotin. This also resulted in the release of
17
18 the amplified DNA product wherein it can repeatedly hybridize with new biotin/Cy5-labeled
19
20 to initiate the next rounds of cleavage. In a similar strategy, mir-196a2C was detected using
21
22 the designed mir-196a2C padlock probes. In the absence of the mir-96a2T, more Cy5/biotin
23
24 capture probes are cleaved, leading to smaller amounts of the intact capture probes that can
25
26 bind on the surface of the streptavidin-coated QD. Consequently, this reduces the FRET
27
28 between the QD donor and Cy5 acceptors, resulting in decreased Cy5 counts being detected
29
30 in the single-particle FRET detection measurement. On the other hand, the mir-196a2T-
31
32 specific linear padlock probe cannot be circularized in the absence of mir-196a2T. Under
33
34 these conditions, RCA amplification and cleaving reactions will happen. Hence, the
35
36 biotin/Cy5-labeled capture probe remains intact which can bind to the QD surface *via*
37
38 specific streptavidin-biotin interactions, resulting in strong QD sensitised Cy5 FRET signal.
39
40
41
42
43
44
45
46
47
48
49
50
51
52
53
54
55
56
57
58
59
60

With the integration of the PG-RCA reaction and nicking enzyme-driven recycling

1
2
3
4 amplification, this QD-based miRNA nanosensor exhibited an impressive detection limit of
5
6
7 50.9 aM and a large dynamic range of 7 orders of magnitude from 0.1 fM to 1 nM for the
8
9
10 specific microRNA target. Moreover, this assay can even distinguish variant frequencies
11
12
13 down to as low as 0.001% in the mixtures of mir-196a2C and mir196a2T. Importantly, this
14
15
16 QD-based miRNA nanosensor can be used to analyse the point mutation of mir-196a2 in the
17
18
19 lung tissues of NSCLC patients, holding great potentials for further applications in
20
21
22 biomedical research and clinical diagnosis presumably in the clinical laboratory settings. Its
23
24
25 complex signal amplification and assay procedures together with a relatively complex single-
26
27
28 particle counting readout method may, however, limit its use in applications that require rapid
29
30
31 results.

32 33 (v) Nanomaterial assisted signal amplification

34
35
36 In signal amplification, nanomaterials are often functionalised with biomolecules for
37
38
39 target-specific recognitions and/or carrying high loads of signal moieties, catalysts, optical
40
41
42 emitters, and electronic conductors. Biofunctionalised nanomaterials can amplify the signal
43
44
45 transduction events due to their capability of direct interaction with their target, allowing for
46
47
48 detection of biomolecules down to the single-molecule level [79]. Signal amplification can
49
50
51 eliminate some special requirements of the target/probe amplification schemes such as the
52
53
54 need of enzymes and thermal cycles (*ca.* PCR). As a result, this can simplify experimental
55
56
57 protocols, lower the assay cost, and provide amenability to miniaturisation. Hence, the use of
58
59
60

1
2
3
4 biofunctionalized nanomaterials for signal amplification has been very attractive in the
5
6
7 development of ultrasensitive DNA assays without the need of target and probe
8
9
10 amplifications. The following section presents some ultrasensitive detection of SNPs
11
12
13 achieved through use nanomaterials for signal amplification.

5.1 Nanoparticle Bio-barcode Amplification

14
15
16
17
18
19
20
21 An excellent example of the earlier developments here is the Bio-barcode assay
22
23
24 developed by the Mirkin group [80]. It uses a short DNA-modified Au NP tagged with
25
26
27 hundreds of copies of the bio barcode DNAs (Bbc-Au NP) as signal probe, and another
28
29
30 DNA-modified magnetic microparticle (Oligo-MMP) as capture probe (Fig. 8). The two
31
32
33 DNAs are complementary to each half of the target DNA, so that they can sandwich bind to
34
35
36 the target DNA, forming a Bbc-Au NP/DNA target/Oligo-MMP hybrid structure. After
37
38
39 magnetic separation and washing to remove any unbound species, thermal denaturation of the
40
41
42 hybrid releases the bio barcode DNAs, converting each capture DNA target into hundreds of
43
44
45 copies of barcode DNAs. These are then detected by a sensitive scanometric assay coupled
46
47
48 with silver amplification to achieve ultrasensitivity [81]. This assay provides an impressive
49
50
51 label-free detection of target DNA down to 500 zM, comparable to many PCR based methods
52
53
54 [80]. It can also discriminate the perfect match DNA from the SNP target. Although its
55
56
57 relatively modest discrimination ratio, $\sim 3:1$, may limit its capability of detecting low
58
59
60

1
2
3
4 abundant SNP targets in wild-type gene background.
5
6
7
8

9
10 *5.2 Signal Amplification using labeled and enriched nanoparticle probes*
11

12
13 Metallic nanoparticles can be employed as scaffold for loading not only the capture but
14 also signal molecules. These labelled nanoparticles present an important signal amplification
15 strategy as they can directly enhance the readout signal for each target and probe recognition
16 while retaining a high binding specificity. Over the past few years, silica particles have been
17 used as another carrier platform due to their large surface areas, well-known surface
18 chemistries and good biocompatibility.
19

20
21 Wu and colleagues have reported a labeling-based signal amplification strategy for
22 ultrasensitive detection of target DNA using QD assembled SiO₂ microspheres [82]. This
23 method is used as an indirect method for ultrasensitive detection of HIV DNA using hydride
24 generation atomic fluorescence spectrophotometry [HG-AFS]. This assay involves the use of
25 sandwich hybridization between the target DNA, biotin-capture probe and streptavidin tagged
26 QD-SiO₂ assembly, converting each captured DNA target into thousands of SiO₂ tagged QDs.
27
28 After acid dissolution of the QDs, the resulting Cd²⁺ ions were detected by HG-AFS, giving a
29 highly impressive detection limit of 0.8 aM for the target DNA and a dynamic range of 3
30 orders of magnitude (from 1 aM to 1 fM). The outstanding sensitivity suggests that the HG-
31
32 AFS method is suitable for the ultrasensitive biosensing.
33
34
35
36
37
38
39
40
41
42
43
44
45
46
47
48
49
50
51
52
53
54
55
56
57
58
59
60

1
2
3
4 An ultrasensitive chemiluminescent method using Au NP based signal amplification has
5
6 recently been developed by Zhang and colleagues [83]. Using the Watson-Crick base pairing,
7
8 a guanine monomer modified Au NP probe is coupled to the cytosine mutated DNA duplex in
9
10 the presence of DNA polymerase I. Each guanine modified Au NP probe is also linked to 77
11
12 CuS NPs which act as signal generator. After acid dissolution of the CuS NPs, the released
13
14 Cu^{2+} ions are coordinated to cyanides to form $[\text{Cu}(\text{CN})_4]^{2-}$ complexes. These are then reacted
15
16 with luminol to give rise to chemiluminescence signal for target DNA quantification. A
17
18 further improvement in the signal sensitivity is achieved by incorporating a pre-concentration
19
20 of Cu^{2+} ions by anodic stripping voltammetry (ASV). These have enabled this assay to
21
22 achieve a low detection limit of 19 aM for one base mutant DNA and a linear range of 80 aM
23
24 to 10 fM.
25
26

27
28 The labeling of the target DNA with a large number of signal generators coupled with
29
30 sensitive electrochemiluminescence detection is very powerful towards ultrasensitivity for
31
32 SNP detection as demonstrated by the Willner group [84]. In this assay, a mutant DNA with
33
34 one base mismatch (C→G mutation) is first hybridised to a complementary DNA modified
35
36 magnetic NP. It is then treated with a DNA polymerase in the presence of biotin-dCTP and
37
38 other dNTPs. This is then followed by multiple thermal cycles of dissociation, annealing and
39
40 labeling, resulting in poly-labeling of the magnetic NPs with biotins. After magnetic
41
42 separation and treatment with avidin-horseradish peroxidase (Avidin-HRP), the resulting
43
44
45
46
47
48
49
50
51
52
53
54
55
56
57
58
59
60

1
2
3
4 avidin-HRP functionalised magnetic NPs and naphthoquinone NPs are deposited on an
5
6 electrode guided by an external magnetic field. Applying an electric potential reduces
7
8 naphthoquinone to hydroquinone, which simultaneously reduces O₂ to H₂O₂, triggering the
9
10 HRP catalysed oxidation of luminol and yielding a chemiluminescence signal. Under
11
12 optimized conditions, this assay has reported an impressive sensitivity of 8.3 aM for the
13
14 M13φ DNA (50 copies in 10 μL sample) and 10 aM for a mutant DNA.
15
16
17
18
19
20

21
22 Despite showing impressive sensitivities, none of the above ultrasensitive assays have
23
24 reported the simultaneous detection of multiple targets. Further developments on the
25
26 multiplexing capability of an SNP assay are highly desirable for improving the diagnostic
27
28 accuracy. Recently, Gambari and colleagues [85] have reported the direct detection of SNPs
29
30 in non-amplified human genomic DNA carrying the mutated β⁰39-globin gene sequence by
31
32 using surface plasmon resonance imaging (SPRI). This gene is involved in the hereditary
33
34 blood disorder diseases known as β-thalassemia. The detection is achieved by using Au NP
35
36 conjugated with multiple copies of DNA β⁰39, an 11-mer oligonucleotide. Prior to analysis,
37
38 the surfaces of 6 microfluidic channels are modified with PNA-N and PNA-M probes whose
39
40 nucleic acid sequences are complementary to the normal and mutant genes respectively (Fig.
41
42 9). The samples are directly fluxed into these channels to allow the direct hybridisation
43
44 between each of the samples (*e.g.* normal βN/βN; homozygous β⁰39/β⁰39 and heterozygous
45
46 β⁰39/βN) on PNA functionalized surfaces. The SPRI responses between the samples and the
47
48
49
50
51
52
53
54
55
56
57
58
59
60

1
2
3
4 two different PNA probes are used as controls. Subsequently, the conjugated Au NPs are
5
6
7 fluxed into the microchannels and captured by specific hybridization between their surface
8
9
10 DNA β^039 strands and exposed target DNA sequence not involved in binding to the PNA
11
12
13 probes, allowing for greatly enhanced SPRI signal. This assay has achieved the sensitive
14
15
16 detection of genomic DNAs down to 2.6 aM ($5 \text{ pg } \mu\text{L}^{-1}$) without PCR amplification. It can
17
18
19 also discriminate between the normal, homozygous β^039/β^039 , and heterozygous $\beta^039/\beta\text{N}$
20
21
22 sequences, albeit with a relatively modest discrimination ratio.
23
24
25
26
27

28 *5.3 Signal Amplification using functionalized nanocontainers*

29
30 The use of nanomaterials with hollow structures for encapsulation of signaling elements
31
32
33 is another attractive strategy for ultrasensitive biosensing. Lin and colleagues [48] have used
34
35
36 a similar base-pairing mechanism to target DNA point mutations using a novel signal
37
38
39 amplification strategy. It uses DNA polymerase I (Klenow fragment) to couple a guanine-
40
41
42 modified NP probe to the mutation site of a duplex DNA. The signal enhancement is
43
44
45 achieved by incorporating Cd^{2+} ions inside an engineered protein with a hollow cage of
46
47
48 interior cavity diameter of 8 nm. This NP probe is also modified with guanine nucleotide to
49
50
51 specifically pair with cytosine point mutation in the DNA duplex. As a result, hybridization of
52
53
54 the mutant DNA (cytosine point mutation) and the biotin-labeled DNA probe forms a stable
55
56
57 duplex DNA structure which is then captured by avidin-modified magnetic NPs. The Cd^{2+}
58
59
60

ions released from the nanoparticle cavity is then detected electrochemically by square wave voltammetry. This assay is sensitive, allowing for detection of 21.5 attomol mutant DNA and can detect SNPs down to frequencies as low as 0.01.

Recently, Zhang and colleagues [86] has developed a new approach using QD-based SNP detection without the need for target or probe amplification. This assay uses a reporter probe modified-liposome (liposome-QD-reporter probe; L@QD complex) serving as a “nano- container” for encapsulation of hundreds of QDs. The presence of the target DNA (T-DNA) and capture probe modified magnetic bead (CP-MB) lead to sandwich hybridization, forming a liposome-QD-reporter probe/T-DNA/CP-MB hybrid structure which is then separated magnetically. The subsequent disruption of liposome-QD complexes results in release of the encapsulated QDs, which are sensitively detected by single-particle counting (Fig.10). An advantage of this approach is that each pair of reporter/capture probes can be encoded with a different coloured QD, allowing for easy detection of multiple DNA targets simultaneously.

As shown in Fig. 10, the presence of HIV-1 only produces fluorescence bursts from the green QDs but not the red QDs. In contrasts, the presence of HIV-2 only produces red QD fluorescence, but not green QD, and thus indicating high assay specificity. Multiplexing has been achieved by encapsulating red and green QDs into the respective reporter probe 1 and reporter probe 2 tagged liposomes, whereupon specific sandwich hybridization lead to the

1
2
3
4 formation of specific magnetic bead-liposome complexes. After magnetic separation, the use
5
6 of two different coloured liposome-QD complexes has enabled the simultaneous detection
7
8 of the HIV-1 and HIV-2 genes (Fig. 10 B-C). The great target amplification (each captured
9
10 DNA targeted is converted into several hundreds of QDs) coupled with sensitive single-
11
12 particle counting method has enabled this assay to be ultrasensitive, with detection limits
13
14 down to 1 and 2.5 aM for HIV-1 and for HIV-2, respectively. With the judicious design of
15
16 capture and signal probes, this assay may provide an ultrasensitive approach for
17
18 simultaneous detection of multiple DNA targets. However, this assay is unlikely to be able
19
20 to provide high enough SNP discrimination ratio useful for detection of specific low
21
22 abundant SNPs in wild-type gene background because of the small stability difference of the
23
24 sandwich DNAs for the wild-type and SNP DNAs formed with the reporter/capture probes.
25
26 Its single-particle counting readout strategy may also limit its application in resources poor
27
28 environment.
29
30
31
32
33
34
35
36
37
38
39
40
41
42

43 *5.4 Signal Amplifications using enzyme guided crystal growth*

44 Stevens and colleagues have recently developed a novel plasmonic nanosensor that
45
46 works on a principle of inverse sensitivity signal-generation mechanism, [87-88] where an
47
48 amplified signal is observed when less target molecules are present. The inverse sensitivity
49
50 procedure is achieved using glucose oxidase (GOx) which catalyses the generation of
51
52 hydrogen peroxide to tailor the plasmonic response of the gold nanosensors. Depending on
53
54
55
56
57
58
59
60

1
2
3
4 the concentration, GOx can control the *in-situ* rate of nucleation of nascent Ag nanocrystals
5
6 or Ag coating on Au nanostars, resulting in variations of the localized surface plasmon
7
8 resonance (LSPR). At low GOx concentration, a low supply of H₂O₂ favours the deposition
9
10 of a homogeneous silver coating on the Au nanostars, leading to blueshift of the LSPR band.
11
12 Whereas a high GOx concentration favours the nucleation of silver nanocrystals instead of
13
14 depositing on Au nanostars, leading to less LSPR shifts (Fig. 11). This principle is used to
15
16 develop a plasmonic ELISA using a GOx conjugated antibody in a typical sandwich immune-
17
18 binding format. The concentration of GOx is directly related to the target concentration.
19
20 Prostate specific antigen (PSA) and HIV-1 capsid antigen p24 are used as model protein
21
22 targets in whole serum conditions. This assay has demonstrated an extremely impressive
23
24 sensitivity of 40 zM [87] and 1 aM [88] for PSA and HIV-1 capsid antigen, respectively.
25
26 Moreover, the assay results can be directly visualised by the naked eye, and therefore offers a
27
28 simple, highly attractive alternative to the costly nucleic acid-based HIV infection diagnosis
29
30 test. In principle, it can be adapted for the detection of any analyte with a suitable antibody,
31
32 making it a versatile tool for ultrasensitive diagnostics. Despite of great simplicity and
33
34 ultrasensitivity, the plasmonic ELISA however, has a rather small dynamic range of one order
35
36 of magnitude, making it difficult to quantify the exact target concentration.
37
38
39
40
41
42
43
44
45
46
47
48
49
50
51
52
53
54
55

56 Conclusion and Outlook

57
58
59
60

1
2
3
4 Significant advances have been made over the past few years in the development of
5
6
7 PCR-free assays suitable for specific and ultrasensitive detection of SNPs. The incorporation
8
9
10 of various biofunctionalised nanomaterials coupled with novel amplification strategies have
11
12
13 permitted the detection of extremely low concentrations of SNPs, down to the aM - zM
14
15
16 range. Such levels of sensitivity have already compared very favorably with many PCR based
17
18
19 methods. In general, the amplification strategies may be classified as one of the following
20
21
22 categories:

- 23
24 (i) Nanoparticle–target assisted PCR amplification.
25
26
27 (ii) Nanoparticle-target assisted probe amplification.
28
29
30 (iii) Target recycling coupled with probe and/or signal amplification.
31
32
33 (iv) Tandem amplification schemes and signal catalytic cascades.
34
35
36 (v) Nanomaterial enhanced signal amplification.
37

38
39 In general, the sensitivity of a nanomaterial-based SNP assay can be greatly enhanced by
40
41
42 combining target, probe and signal amplification schemes. Most of the recent target and
43
44
45 probe amplification schemes have exploited the great catalytic power and specificity of
46
47
48 enzymes to achieve ultra-sensitivity and specificity. Of particular interest here is the use of
49
50
51 DNAzymes that can undergo the so-called enzymatic cascade reactions, where the activation
52
53
54 of multiple enzymes by a target DNA can result in ultra-sensitivity, comparable many PCR
55
56
57 based assays. Another widely used strategy is the use of restriction enzymes that specifically
58
59
60

1
2
3
4 recognise the restriction sites to degrade the reporter probe, allowing for target recycling.
5
6
7 These autocatalytic strategies have resulted in unmatched sensitivities while still maintaining
8
9
10 high specificity. However, a limitation here is that restriction enzymes can only recognize a
11
12
13 specific sequence and therefore are not suitable for universal SNP detection. Several
14
15
16 ingenious ways in the design of nanomaterials for signal amplification strategies have also
17
18
19 been developed, including the use of multiple tagging and enrichment of nanoparticle probes
20
21
22 with signal moieties to enable ultra-sensitivity. Some of these strategies also hold great
23
24
25 promises for multiplexed detection, an important property for high diagnostic accuracy.
26

27
28
29 Despite significant advances, several limitations still need to be resolved before they can
30
31
32 be translated into clinical diagnostic assays. For example, although a number of assays have
33
34
35 reported aM, even zM sensitivity, most of which were still at the proof-of-concept stage and
36
37
38 were carried out under clean buffers. They have not yet been tested in clinically related
39
40
41 media, such as blood, serum, saliva and urine. Furthermore, most assays have reported a
42
43
44 rather limited SNP discrimination ratio (< 10 fold), making them potentially unsuitable for
45
46
47 detection of low abundant disease related SNPs in the background of wild-type gene/genomic
48
49
50 DNA because of the strong interference from the background DNAs. Moreover, the lack of
51
52
53 the multiplexing capability could pose a significant limiting factor for the real clinical
54
55
56 potential. The stability of the biofunctionalised nanomaterials is another important issue for
57
58
59 such nano-enabled SNP biosensors. In this regard, the fundamental understanding of the
60

1
2
3
4 biomolecule-nanomaterial interactions is imperative to alleviate problems of high background
5
6
7 signals due to non-specific adsorptions in serum and/or other complex clinical samples.
8

9
10 The use of biofunctionalised nanomaterials together with novel amplification strategies
11
12 has transcended barriers to the attainment of extremely low detection limits of disease-related
13
14 SNPs. This ultimately ushers the way for more practical concerns such as the realistic
15
16 applications of the technology in clinical settings. Even more challenging is the development
17
18 of a robust, portable, point-of-care diagnostic system that can specifically detect the ultralow
19
20 level of disease-related SNPs rapidly and conveniently on the site of the patient and in places
21
22 such as the doctor's office, school clinic and in patients' residence [89].
23
24
25
26
27
28
29

30 These also calls for improving the assays' amenability towards automation and
31
32 miniaturization because most current assays still require the use of expensive and complex
33
34 instrumentation and complex procedures, limiting their potential in rapid diagnosis. Electro-
35
36 chemical signal transduction can provide an option for the miniaturization and automation but
37
38 these methods are prone to false positives [26]. The recent advances in microfluidics [90-91]
39
40 may be able to address sample throughput and automation challenges in SNP assays. If all of
41
42 these challenges were met, the automation of these ultrasensitive assays may lead to the
43
44 integration of sample processing, quantification and signal measurement in an all-in-one
45
46 device in real clinical setting. This would greatly facilitate the rapid, accurate disease
47
48 diagnosis and prognosis. In view of this, these are still crucial challenges that need to be
49
50
51
52
53
54
55
56
57
58
59
60

1
2
3
4 addressed, and more efforts will be needed to improve the analytical sensing performance and
5
6 portability of SNP assays.
7
8

9 10 11 12 **Acknowledgement**

13
14 We would like to thank the University of Leeds for funding this project and also for funding
15
16 L.DS.L with the Leeds International Research Scholarship (LIRS) to allow him pursuing his
17
18 PhD studies at University of Leeds. Y.G. would like to thank the Wellcome Trust (UK) for
19
20 providing her a Career Re-entry Fellowship (Grant No: 097354/Z/11/Z).
21
22
23
24
25
26
27

28 29 **References**

- 30
31 [1] See the Human Genome Project website: <http://www.genome.gov/10001772>, Date retrieved:
32 November 1, 2014.
33
34 [2] D. G. Wang, *et al.*, *Science*, 1998, **280**, 1077-1082
35
36 [3] H. C. Erichsen and S. J. Chanock, *Brit. J. Cancer*, 2004, **90**, 747 – 751.
37
38 [4] D. Botstein and N. Risch, *Nat. Genet.*, 2003, **33**(Suppl), 228 – 237.
39
40 [5] C. S. Carlson, *et al.*, *Nat. Genet.*, 2003, **33**, 518 – 521.
41
42 [6] M. Monot *et al.*, On the origin of leprosy, *Science*, 2005, **308**, 1040-1042.
43
44 [7] D. Zhang, J. Ma, K. Brismar, S. Efendic, and H. F. Gu, *J. Diab. Complic.*, 2009, **23**, 265-272.
45
46 [8] Y. Suh and J. Vijg, *Mut. Res.* 2005, **573**, 41-53.
47
48 [9] B. N. Chorley, X. Wang, M. R. Campbell, G. S. Pitman, M. A. Noureddine, and D. A. Bell, *Mut.*
49 *Res.* 2008, **659**, 147-157.
50
51 [10] J. Robert, V. Le Morvan, D. Smith, P. Pourquier, and J. Bonnet. *Crit. Rev. Oncol. Hematol.*,
52 2005, **54**, 171-196.
53
54 [11] B. Rahim-Williams, J. L. Williams, and R. B. Fillingim, *Pain Med.*, 2012, **13**, 522-540.
55
56 [12] J. Liu, C. He, C. Xing, and Y. Yuan, *Mut. Res.* **2014**, 765, 11-21.
57
58 [13] A. Figl *et al.*, *Mut. Res.*, 2009, **661**, 78-64.
59
60 [14] C. M. Oliveria, K. D. Hadfield, A. K. Siriwardena, and W. Newman, *Pancreas*, 2012, **41**, 428-
434.
[15] J. M. Ostrem, U. Peters, M. L. Sos, J. A. Wells, and K. M. Shokat, *Nature*, 2013, **503**, 548-551.

- 1
2
3 [16] O. I. Sentina, T. V. Byzova, J. C. Adams, J. J. McCarthy, E. J. Topol, and E. F. Plow, *Int. J.*
4 *Biochem Cell Biol.*, 2004, **36**, 1013-1030.
5
6 [17] F. Coppedè, C. Armani, D. D. Bidia, L. Petrozzi, U. Bonuccelli, and L. Migliore. *Mut. Res.* 2005,
7 **579**, 107-114.
8
9 [18] B. Roy, N. Maksemous, R. A. Smith, S. Menon, G. Davies, and L. R. Griffiths, *Mut. Res.* 2012,
10 **732**, 3-8.
11
12 [19] Z. Hu, J. Chen, T. Tian, X. Zhou, H. Gu, L. Xu, Y. Zeng, R. Miao, G. Jin, H. Ma, Y. Chen and
13 H. Shen, *J. Clin. Invest.*, 2008, **118**, 2600-2608.
14
15 [20] B. M. Ryan, A. I. Robles and C. C. Harris, *Nat. Rev. Cancer*, 2010, **10**, 389-402.
16
17 [21] M. M. Mhlanga, and L. Malmberg, *Methods*, 2001, **25**, 463-471.
18
19 [22] Y. V. Gerasimova and D. M. Kopaschchikov, *Chem. Soc. Rev.*, 2014, **43**, 6405-6438.
20
21 [23] L. J. Chin, E. Ratner, S. Leng, R. Zhai, S. Nallur, I. Babar, R. U. Muller, E. Straka, L. Su, E.
22 A. Burki, R. E. Crowell, R. Patel, T. Kulkarni, R. Homer, D. Zelterman, K. K. Kidd, Y. Zhu,
23 D. C. Christiani, S. A. Belinsky, F. J. Slack and J. B. Weidhaas, *Cancer Res.*, **2008**, **68**,
24 8535.
25
26 [24] J. M. Butler (2012), Single nucleotide polymorphisms and applications In *Advanced Topics*
27 *in Forensic DNA Typing* (pp.347-369), California, USA: Academic Press.
28
29 [25] R. M. Twyman (2009), Single nucleotide polymorphism analysis In *Encyclopedia of*
30 *Nueroscience* (pp. 871-875), California, USA: Academic Press.
31
32 [26] M. L. Ermini, S. Mariani, S. Scarano, and M. Minunni, *Biosens. Bioelec.*, 2014, **61**, 28-35.
33
34 [27] P. D. Howes, S. Rana, and M. M. Stevens, *Chem. Soc. Rev.*, 2014, **43**, 3835-3853.
35
36 [28] W. Shen, C.L. Lim, and Z. Gao, *Chem. Commun.*, 2013, **49**, 8114-8116.
37
38 [29] X. Chen, A. Ying, and Z. Gao, *Biosens. Bioelec.*, 2012, **36**, 89-94.
39
40 [30] C. Bui *et al.*, (2010), Enzymatic and chemical cleavage methods to identify genetic variation
41 In *Molecular Diagnostics* (pp. 29-44), London, California, USA: Academic Press.
42
43 [31] H. Zhang, X. Fu, L. Liu, Z. Zhu, and K. Yang, *Anal. Biochem.*, 2012, **426**, 30-39.
44
45 [32] F. Kakihara, Y. Kurebayashi, Y. Tojo, H. Tajima, S. Hasegawa, and M. Yohda, *Anal.*
46 *Biochem.*, 2005, **341**, 72-88.
47
48 [33] H.-A. Ho, K. Dore', M. Boissinot, M. G. Bergeron, R. M. Tanguay, D. Boudreau, and M.
49 Leclerc, *J. Am. Chem. Soc.*, 2005, **127**, 12673-12676.
50
51 [34] H.-A.; Ho, M. Boissinot, M. G. Bergeron, G. Corbeil, K. Dore', D. Boudreau, and M.
52 Leclerc, *Angew. Chem., Int. Ed.*, 2002, **41**, 1548 -1551.
53
54 [35] S. Wang, and G. C. Bazan, *Adv. Mater.* 2003, **15**, 1425-1428.
55
56 [36] B. Liu, S. Baudrey, L. Jaeger, and G. C. Bazan, *J. Am. Chem. Soc.* 2004, **126**, 4076-4077.
57
58 [37] B. Liu, and G. C. Bazan, *Chem. Mater.* 2004, **16**, 4467-4476.
59
60 [38] S. W. Thomas III, G. D. Joly, and T. M. Swager, *Chem. Rev.*, 2007, **107**, 1339-1386.
[39] J. Garcia, Y. Zhang, H. Taylor, O. Cespedes, M. E. Webb, and D. Zhou, *Nanoscale*, 2011, **3**,

3721-3730.

- [40] W. Shen, H. Deng, and Z. Gao, *J. Am. Chem Soc.*, 2012, **134**, 14678-14681.
- [41] L. Qui, L. Qiu, H. Zhou, Z. Wu, G. Shen, and R. Yu, *New J. Chem.*, 2014, **38**, 4711-4715.
- [42] W. Xu, X. Xie, D. Li, Z. Yang, T. Li and X. Liu, *Small*, 2012, **8**, 1846-1850.
- [43] L. Tang, I. S. Chun, Z. Wang, J. Li, X. Li, and Y. Lu, *Anal. Chem.*, 2013, **85**, 9522-9527.
- [44] C. H. Liu, Z. P. Li, B. A. Du, X. R. Duan, and Y. C. Wang, *Anal Chem.*, 2006, **78**, 3738-3744.
- [45] C. Y. Zhang, H. C. Yeah, M. T. Kukori and T. H. Wang, *Nat. Mater.*, 2005, **24**, 826-831.
- [46] H. Ji, F. Yan, J. Lei, and H. Ju, *Anal. Chem.*, 2012, **84**, 7166-7171.
- [47] G. D. Liu, T. M. H. Lee, and J. J. Wang, *J. Am. Chem. Soc.*, 2005, **127**, 38-39.
- [48] G. Liu, and Y. H. Lin, *J. Am. Chem. Soc.*, 2007, **129**, 10394-10401.
- [49] Y. Zhang, C. Pilapong, Y. Guo, Z. Ling, O. Cespedes, P. Quirke, and D. Zhou., *Anal. Chem.*, 2013, **85**, 9238-9244.
- [50] S. Bi, L. Li, and S. Zhang, *Anal. Chem.*, 2010, **88**, 9447-9454.
- [51] F. Patolsky, Y. Weizmann, E. Katz, and I. Willner, *Angew. Chem. Int. Ed.*, 2003, **42**, 2372-2376.
- [52] S. Bi, Z. Zhang, Y. Dong, and Z. Wang, *Biosens. Bioelec.*, 2015, **65**, 139-144.
- [53] Y. Zhang, Y. Guo, P. Quirke, and D. Zhou, *Nanoscale*, 2013, **5**, 5027-5035.
- [54] G. Liu, and Y. Lin, *J. Am. Chem. Soc.*, 2007, **129**, 10394-10401.
- [55] W. Xu, X. J. Xue, T. H. Li., H. Q. Zeng, and X. G. Liu, *Angew. Chem., Int. Ed.*, 2009, **48**, 6849-6852.
- [56] M. Luo, X. Chen, G.H. Zhou, X. Liang, L. Chen, H. Ji. and Z. K. He, *Chem. Commun.*, 2012, **48**, 1126-1128.
- [57] D. Brouard, M. L. Viger, A. G. Bracamonte, and D. Boudreau, *ACS Nano*, 2011, **5**, 1888-1896.
- [58] D. Brouard, O. Ratelle, A. G. Bracamonte, M. St-Loius, and D. Boudreau, *Anal. Methods*, 2013, **5**, 6896-6999.
- [59] D. Brouard , O. Ratelle, J. Perreault, D. Boudreau, and M. St-Louis, *Vox. Sanguinis*, 2015, **108**, 197-204.
- [60] See the U.S.A. National Cancer Institute website,
<http://www.cancer.gov/cancertopics/factsheet/detection/tumor-markers>.
- [61] N. Li, J. Zhang, Y. Liang, J. Shao, F. Peng, M. Sun, N. Xu, X. Li, R. Wang, S. Liu, and Y. Lu, *J. Proteome Res.*, 2007, **6**, 3304-3312.
- [62] L. Yan, J. Zhou, Y. Zheng, A.S. Gamson, B.T. Roembke, S.N. Nakayama, and H.O. Sintim, *Mol. BioSyst.*, 2014, **10**, 970-1003.

- 1
2
3 [63] X. Duan, L. Liu, S. Wang, *Biosens. Bioelec.*, 2009, **24**, 2095-2099.
- 4
5 [64] X. Wu, L. Xu, L. Liu, W. Ma, H. Yin, H. Kuang, L. Wang, C. Xu, N.A. Kotov, *J. Am. Chem. Soc.*,
6
7 2013, **135**, 18629-18636.
- 8
9 [65] W. Ma, H. Kuang, L. Xu, L. Ding, C. Xu, L. Wang, N.A. Kotov, *Nat. Commun.*, 2013, **4**, 2689.
- 10
11 [66] Y. Zhao, L. Xu, W. Ma, L. Wang, H. Kuang, C. Xu, and N. A. Kotov, *Nano Lett.* 2014, **14**, 3908-
12
13 3913.
- 14
15 [67] Z. Zou, Z. Qing, X. He, K. Wang, D. He, H. Shi, X. Yang, T. Qing, and X. Yang, *Talanta*,
16
17 2014, **125**, 306-312.
- 18
19 [68] S. Zhang, Z. Wu, G. Shen, and R. Yu, *Biosens. Bioelec.*, 2009, **24**, 3201-3207.
- 20
21 [69] Y. Cheng, Z. Li, X. Zhang, B. Du, and Y. Fan, *Anal. Biochem.*, 2008, **378**, 123-126.
- 22
23 [70] Y. Chen, M. Yang, Y. Xiang, R. Yuan, and Y. Chai, *Anal. Chim. Acta*, 2013, **796**, 1-6.
- 24
25 [71] C. Cheng, J. Wang, C. yang, Y. Zhou, J. Chen, J. Zhnag, N. Jia, H. Cao, and G. Zhao, *Anal.*
26
27 *Biochem.*, 2013, **434**, 34-38.
- 28
29 [72] A.V. Demchinskaya, I. A. Shilov, A. S. Karyagina, V.G. Lunin, O. V. Sergienko, O.L.
30
31 Voronina, M. Leiser, and L. Plobner, *J. Biochem. Biophys. Meth.*, 2001, **50**, 79-89.
- 32
33 [73] D.A. Giljohan, D.S. Seferos, W.L. Daniel, M.D. Massich, P.C. Patel, and C.A. Mirkin, *Angew.*
34
35 *Chem., Int. Ed.*, 2010, **49**, 3280-3294.
- 36
37 [74] Y. Sato, K. Sato, K. Hosokawa, and M. Maeda, *Anal. Biochem.*, 2006, **355**, 125-131.
- 38
39 [75] D. Kato and M. Oishi, *ACS Nano*, 2014, **8**, 9988-9997.
- 40
41 [76] D. Wu, B-C. Yin, and B.C. Ye, *Biosens. Bioelect.*, 2011, **28**, 232-238.
- 42
43 [77] Y. Cheng, J. Zhao, H. Jia, Z. Yuan, and Z. Li, *Analyst*, 2013, **138**, 2958-2963.
- 44
45 [78] Y. P. Zheng, G. Zhu, X.Y Yang, J.Cao, Z.-L Jing and C.Y. Zhang, *Chem. Commun.*, 2014, **50**,
46
47 7160 – 7162.
- 48
49 [79] J. Lei and H. Ju, *Chem. Soc. Rev.*, 2014, **41**, 2122-2134.
- 50
51 [80] J. M. Nam, S. I. Stoeva, and C. A. Mirkin, *J. Am. Chem. Soc.*, 2004, **124**, 5932-5933.
- 52
53 [81] T. A. Taton, C. A. Mirkin, and R.L. Letsinger, *Science*, 2000, **289**, 1757-1760.
- 54
55 [82] J. Hu, X. Hou, and P. Wu, *J. Anal. At. Spectrom.*, 2015, DOI:10.1039/c4ja00285g
- 56
57 [83] C. Ding, Z. Wang, H. Zhong, and S. Zhang, *Biosens. Bioelec.*, 2010, **25**, 1082-1087.
- 58
59 [84] F. Patolsky, Y. Weizmann, E. Katz, and I. Willner, *Angew. Chem. Int. Ed.*, 2003, **42**, 2372-2376.
- 60
[85] R. D'Agata, G. Breveglieri, L.M. Zanolli, M. Borgatti, G. Spoto and R. Gambari, *Anal. Chem.*,
2011, **83**, 8711–8717.
- [86] J. Zhou, Q.-X. Wang, and C.-Y. Zhang, *J. Am. Chem. Soc.*, 2013, **135**, 2056–2059.
- [87] L. Rodriguez-Lorenzo, R. de la Rica, R. A. Alvarez-Puebla, L.M. Liz-Marzan, and M. M.
Stevens, *Nat. Mater.*, 2012, **11**, 604-607.

1
2
3
4 [88] R. de la Rica and M. M. Stevens, *Nat. Nano.*, 2012, **7**, 821-824.

5 [89] D.A. Giljohann and C.A. Mirkin, *Nature*, 2009, **26**, 461-464.

6
7 [90] C. Zhang and D. Xing, *Chem. Rev.*, 2010, **110**, 4910–4947.

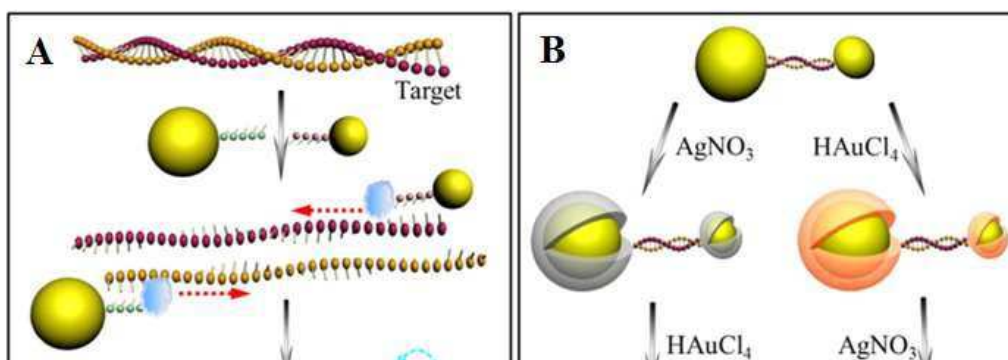
8 [91] J. Zhu, C. Qiu, M. Palla, T. H. Nguyen, J. J. Russo, J. Ju, and Q. Lin, *RSC Adv.*, 2014, **4**, 4269-
9 4277.
10
11
12
13
14
15
16
17
18
19
20
21
22
23
24
25
26
27
28
29
30
31
32
33
34
35
36
37
38
39
40
41
42
43
44
45
46
47
48
49
50
51
52
53
54
55
56
57
58
59
60

Figures and Tables

Table 1: Comparison of the sensing performance of some ultrasensitive nano-enabled DNA detection assays.

First Author Ref.	Nanomaterial Platform	Amplification strategy	Transducer / Analytical Tool	LOD
PCR Based Methods				
Y. Zhao [66]	Au NP + Ag NP	PCR	Circular Dichroism	17 zM
F. Patolsky [84]	Magnetic NP	PCR	Chemiluminescence	8.6 aM
PCR-free Methods				
W. Shen [40]	Au NP	LCR	Colorimetric	20 aM
D. Kato [75]	Au NP and Magnetic NP	LCR	Colorimetric	50 zM
J. Ji [46]	CdTe QD	Target recycling + RCA	Electrochemical	11 aM
S. Bi [50]	Magnetic NP	RCA + DNAzyme	Colorimetric	71 aM
Y.P. Zeng [78]	QD	Primer generation + RCA	Fluorimetric	50.9 aM
J. W. Nam [80]	Au NP + Magnetic NP	Bio-bar-code + silver amplification	Scanometric	0.5 aM
J. Hu [82]	CdS QD	CdS QD loaded in SiO ₂ particles	H ₂ S Generation + Atomic Fluorescence Microscopy	0.8 aM
C. Ding [83]	Au NP + CuS NP	CuS NP loaded Au NP	Electrochemical	19 aM
R. D'Agata [85]	Au NP	Short DNA modified Au NP	Surface Plasmon Resonance Imaging	2.6 aM
J. Zhou [86]	QD	QD entrapped in liposome	Single Particle Counting	1-2.5 aM

PCR: polymerase chain reaction; LCR: ligation chain reaction; LOD: limit of detection.



1
2
3
4
5
6
7
8
9
10
11
12
13
14
15
16
17
18
19
20
21
22
23
24
25
26
27
28
29
30
31
32
33
34
35
36
37
38
39
40
41
42
43
44
45
46
47
48
49
50
51
52
53
54
55
56
57
58
59
60

Fig. 1. Chiroplasmonic core-shell DNA-bridged nanoparticle heterodimers. **(A)** Schematic illustration of the PCR based assembly of Au nanoparticle dimers. **(B)** Deposition of Au and Ag on the DNA-bridged Au nanoparticle dimers leading to single and multiple core-shell heterodimers. **(C)** CD and UV-vis spectra of Au coated heterodimers with DNA concentrations varying from 16 zM to 1.6 pM. **(D)** Calibration curve relating the intensity of CD bands of Au coated heterodimers and the concentration of DNA. Reprinted with permission from ref. 66, copyright © 2014, American Chemical Society.

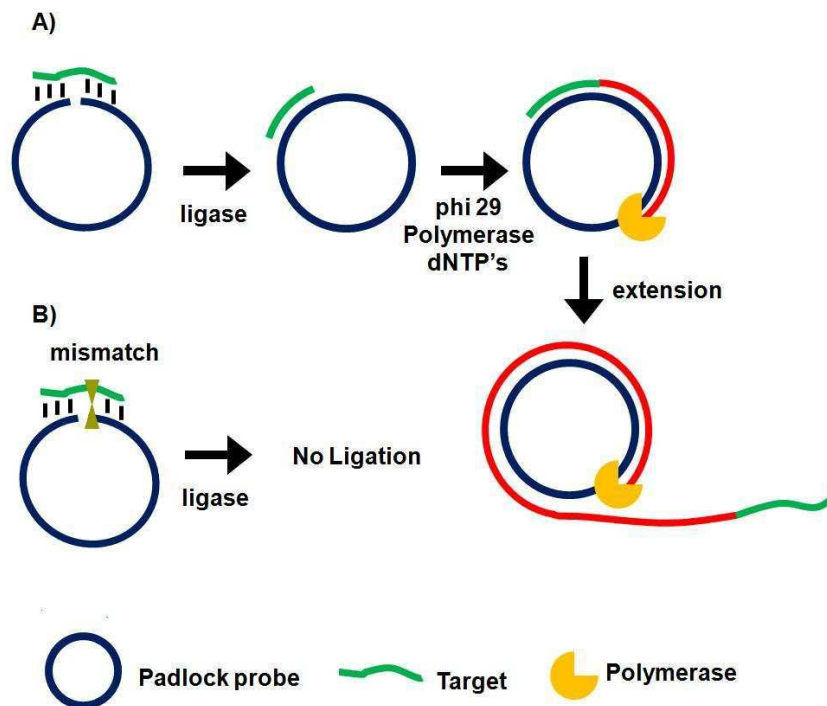


Fig 2. Schematic principle of the rolling cycle amplification and SNP discrimination. **(A)** Hybridization of the perfect-match target DNA to circular padlock probe leads to covalent ligation, producing a target DNA hybridized circular probe where in the presence of phi29 polymerase and dNTP's, the target serves as primer to initiate the circular extension of long single-stranded DNA with repeat sequence complementary to the padlock probe. **(B)** The presence of a single base mismatch between the target DNA to the padlock probe leads to no ligation and hence no amplification.

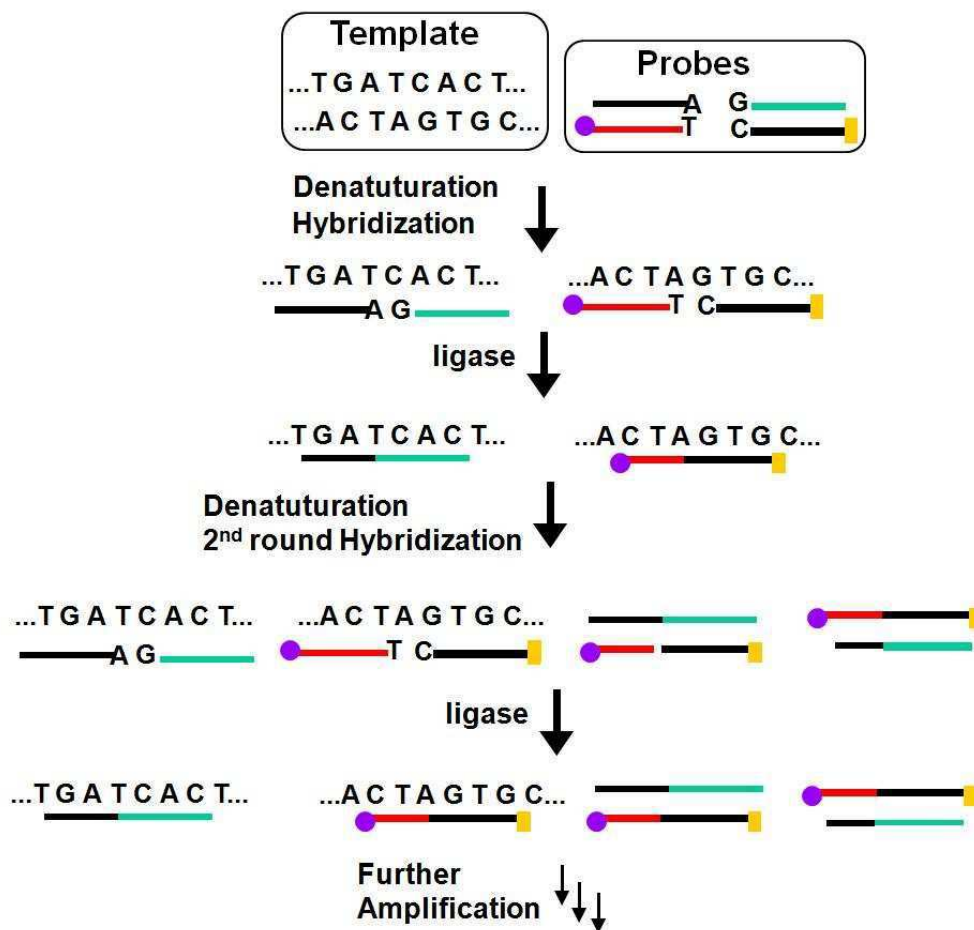




Fig. 3. Schematic principle of the ligase chain reaction (LCR) based DNA amplification strategy. Each of the two DNA strands in the duplex target serves as a template to ligate its respective two short DNA strands, leading to doubling of the ligated product in each cycle and hence an exponential amplification of the target DNA. The amplified target sequences can then be detected by using their specific  and  tags.

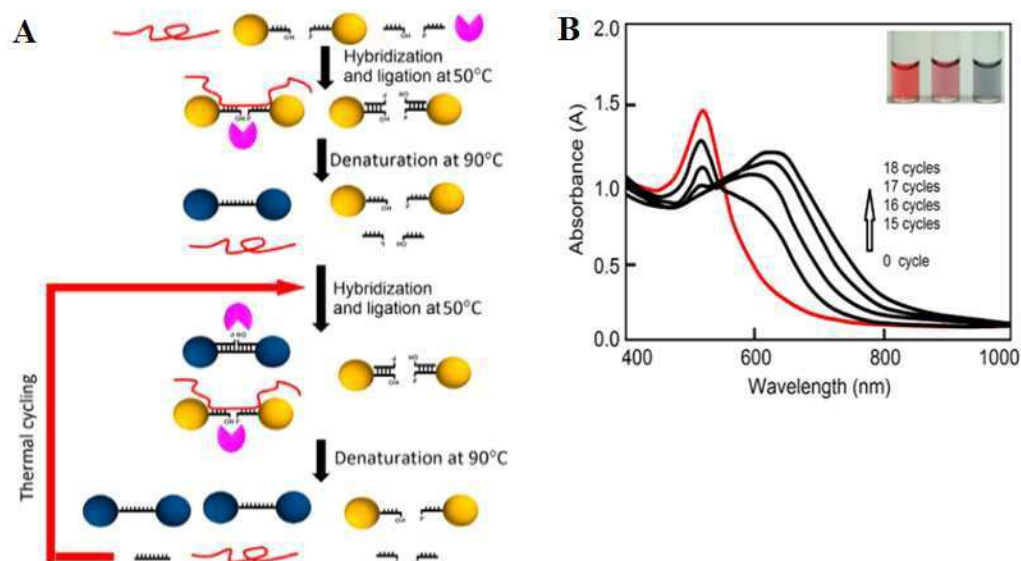


Fig. 4. (A) Schematic illustration of the real-time Au NP mediated LCR assay. (B) UV-Vis spectra of the solution containing 100 fM target DNA and 10 nM CP-coated AuNPs during the LCR process. Inset: color of solution after addition of 0, 5, and 50 nM (left to right) target DNA to 10 nM CP-coated AuNPs. Reprinted with permission from ref. 40, copyright © 2012, American Chemical Society.

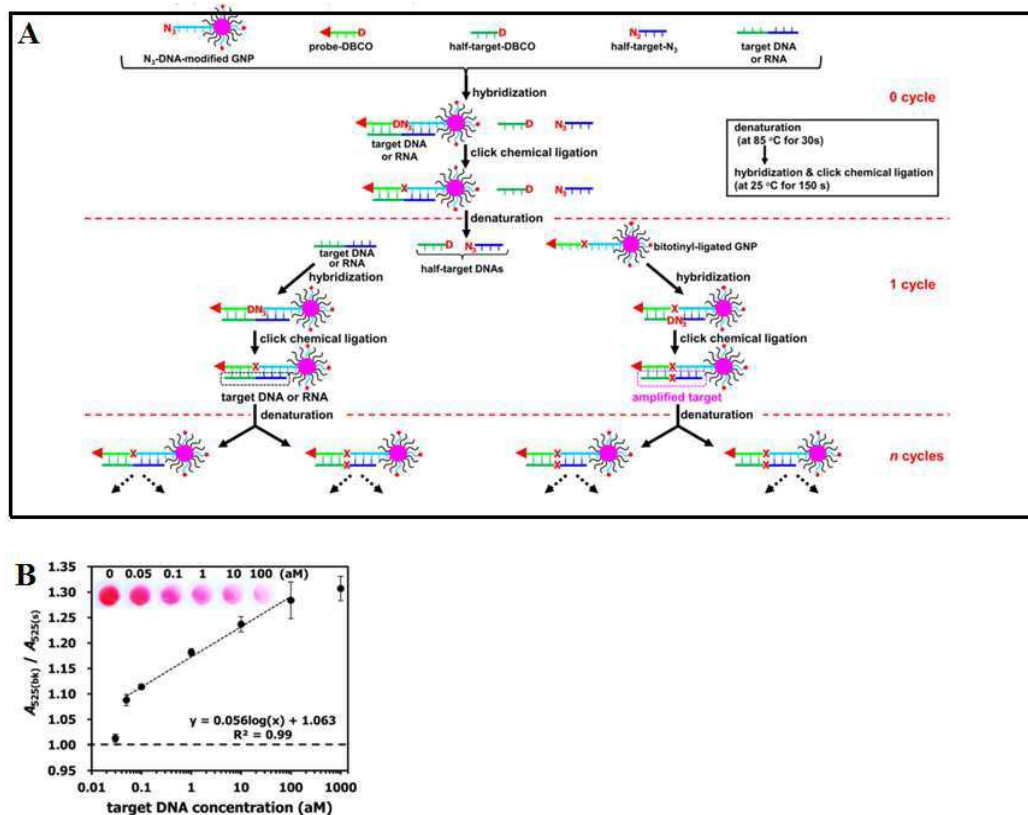


Fig. 5. (A) Schematic illustration of Enzyme Free Click Chemical Ligation on Au nanoparticles involves the hybridization of the target DNA with an azide-modified Au NP (N_3 -AuNP), dibenzocyclooctyne-modified probe (DNCO-probe). (B) A plot of the $A_{525(bk)}/A_{525(s)}$ ratio at different target DNA concentrations using 40 thermal cycles. Inset shows a photograph of the supernatants at different target DNA concentrations. Reprinted permission from ref. 75, copyright © 2014, American Chemical Society.

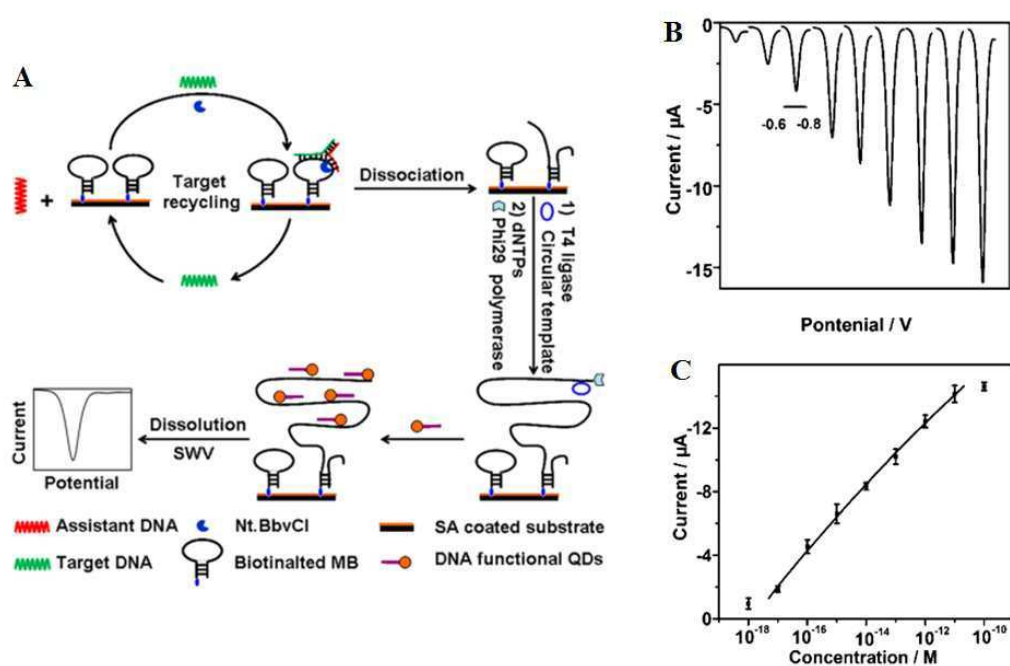


Fig. 6. (A) Schematic illustration of the TEHP amplification strategy for DNA detection, (B) Stripping voltammetric curves of cadmium ions corresponding to (left to right) 10^{-18} , 10^{-17} , 10^{-16} , 10^{-15} , 10^{-14} , 10^{-13} , 10^{-12} , 10^{-11} , and 10^{-10} M of target DNA. (C) The corresponding analytical quantitative dynamic range. Reprinted permission from ref. 46, copyright © 2012, American Chemical Society.

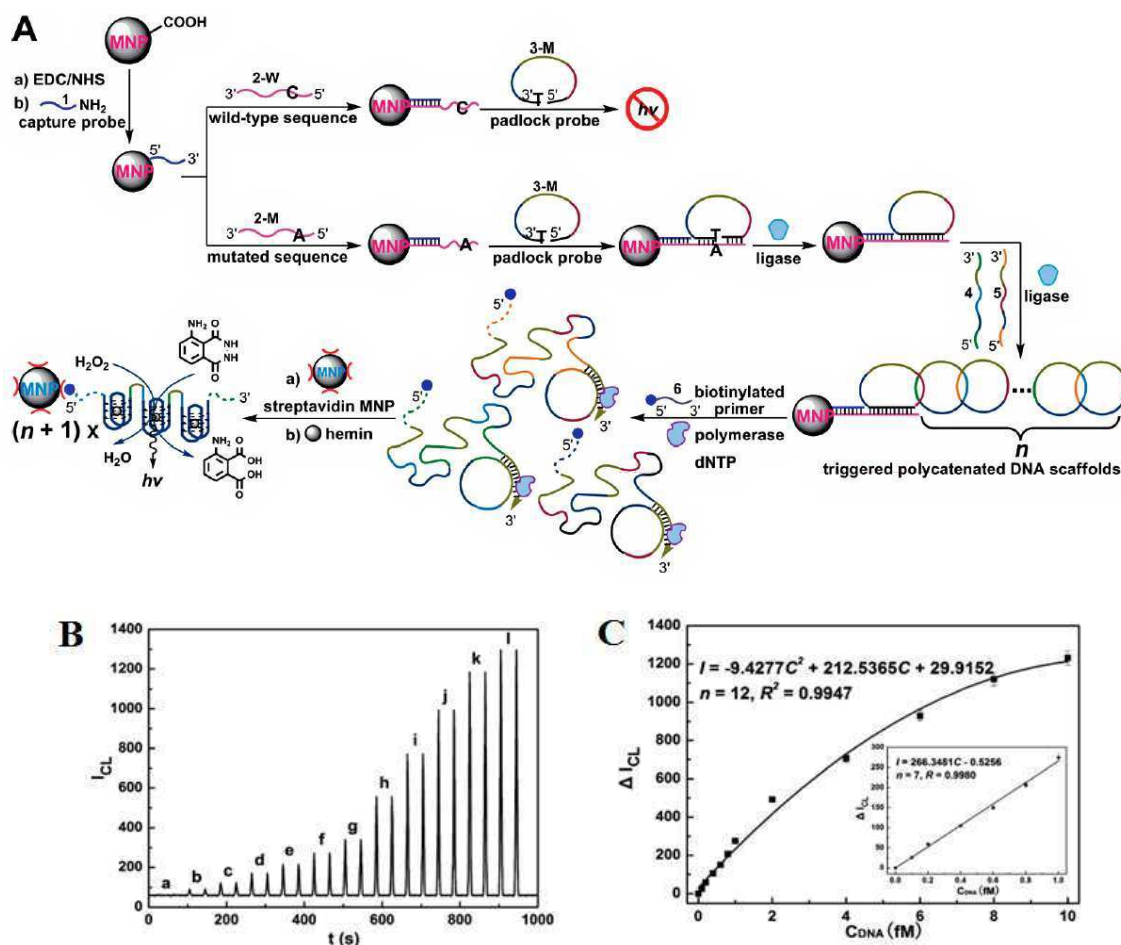


Fig. 7 (A) Schematic representation of interlocked DNA scaffold mediated RCA reaction and DNAzyme amplification assay for the detection of G12C mutation in the KRAS gene. (B) Chemiluminescence signals for the HRP-mimicking DNAzyme-catalyzed luminol- H_2O_2 system corresponding to different concentrations of single-base mutant target DNA: (a) 0; (b) 0.1; (c) 0.2; (d) 0.4; (e) 0.6; (f) 0.8; (g) 1.0; (h) 2.0; (i) 4.0; (j) 6.0; (k) 8.0; (l) 10.0 fM. (C) The corresponding calibration curve of peak height versus the concentration of target DNA. Reprinted with permission from ref. 50, copyright © 2010, American Chemical Society.

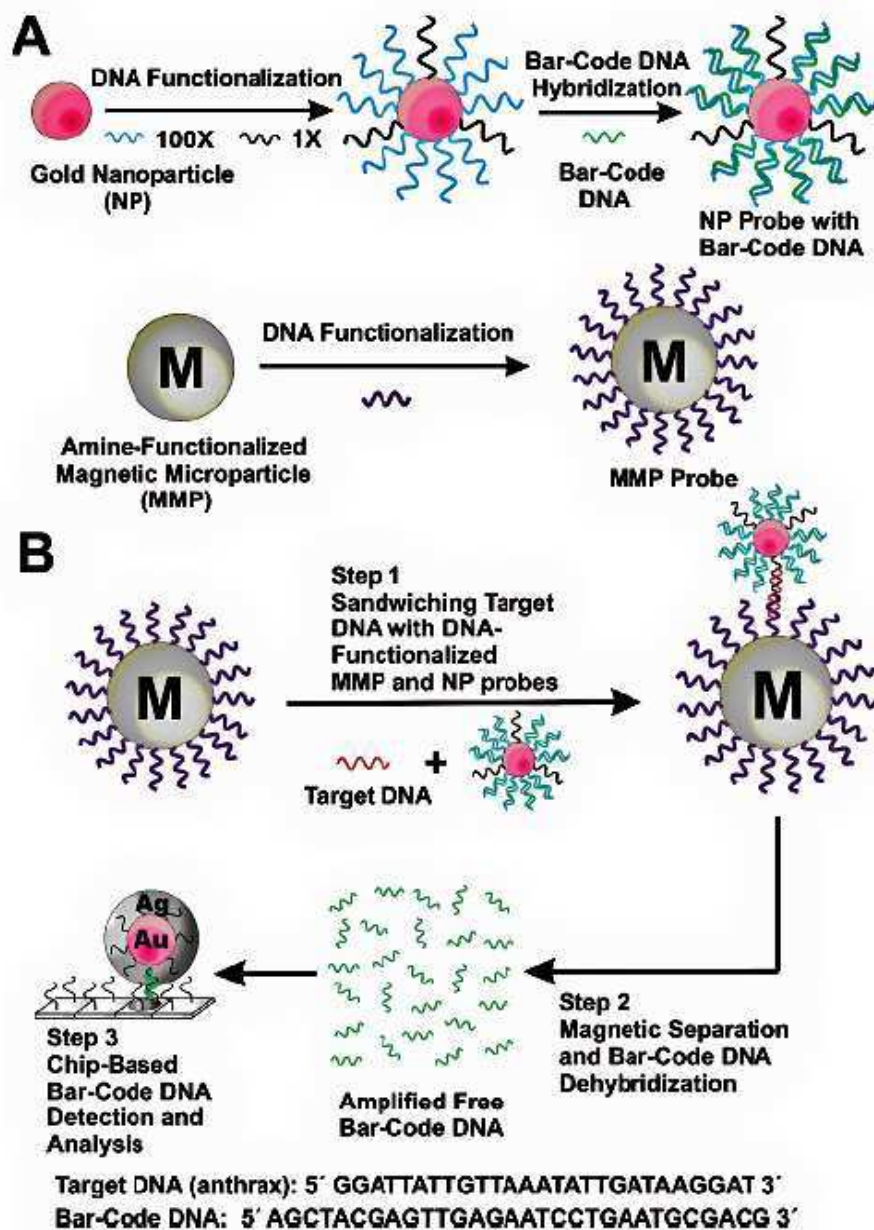


Fig 8. Schematic illustration of the DNA-Bio-bar-code based ultrasensitive assay for DNA detection. (A) The preparation of the DNA modified Au NP and magnetic microparticle probes. (B) Schematics of the nanoparticle-based PCR-free DNA amplification and detection scheme. Reprinted with permission from ref. 80, copyright © 2004, American Chemical Society.

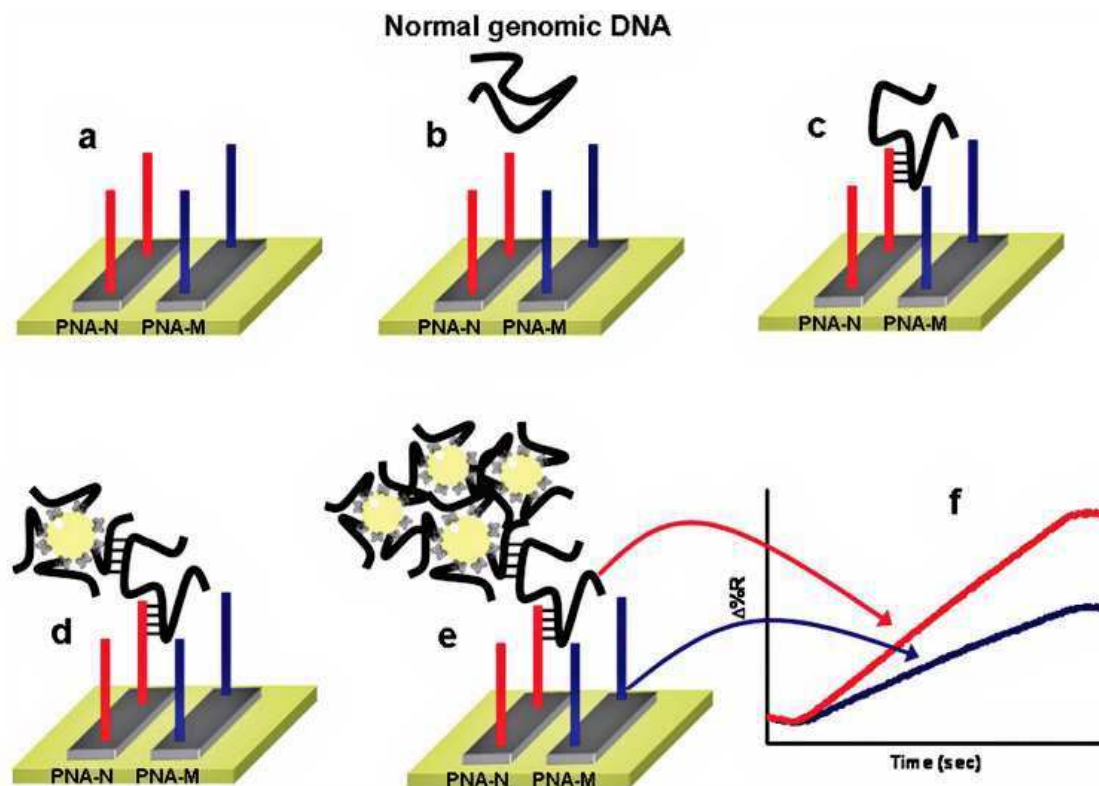


Fig. 9. Schematic illustration of the nanoparticle-enhanced SPRI strategy used to detect the normal β^N/β^N , heterozygous β^{39}/β^N , and homozygous β^{39}/β^{39} genomic DNAs. The PNA-N and PNA-M recognize specifically the normal β -globin and the mutated β^{39} -globin genomic sequences, respectively. Reprinted with permission from ref. 85, copyright © 2011, American Chemical Society.

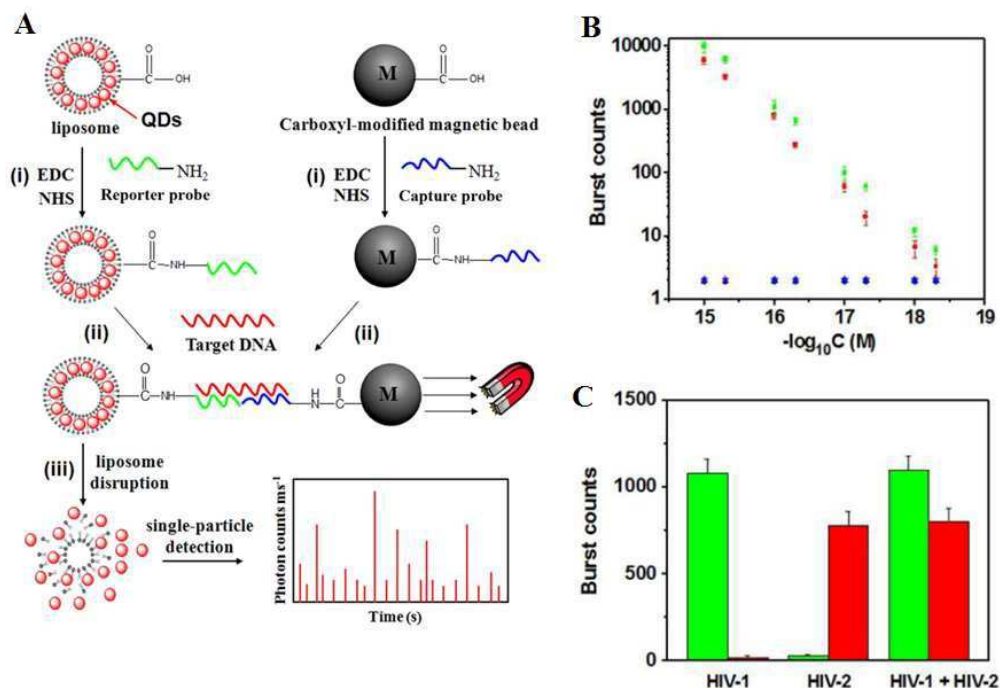


Fig. 10. (A) Schematic illustration for Liposome-QD complexes (L@QD complex) based ultrasensitive detection of attomolar DNA using single-particle detection techniques. The assay involves the sandwich type hybridization of the target DNA to L@QD complex-tagged reporter probes and capture probe modified - magnetic bead. Liposome disruption leads to the release of QD's for single particle detection. (B) A plot of burst counts from the released QDs as a function of the concentrations of HIV-1 (green) and HIV-2 (red). There was no change in the burst counts in the control groups with non-complementary DNA (black and blue), and (C) Simultaneous detection of HIV-1 (green) and HIV-2 (red). The error bars corresponds to standard deviation of three replicates. Reprinted with permission from ref. 86, copyright © 2013, American Chemical Society.

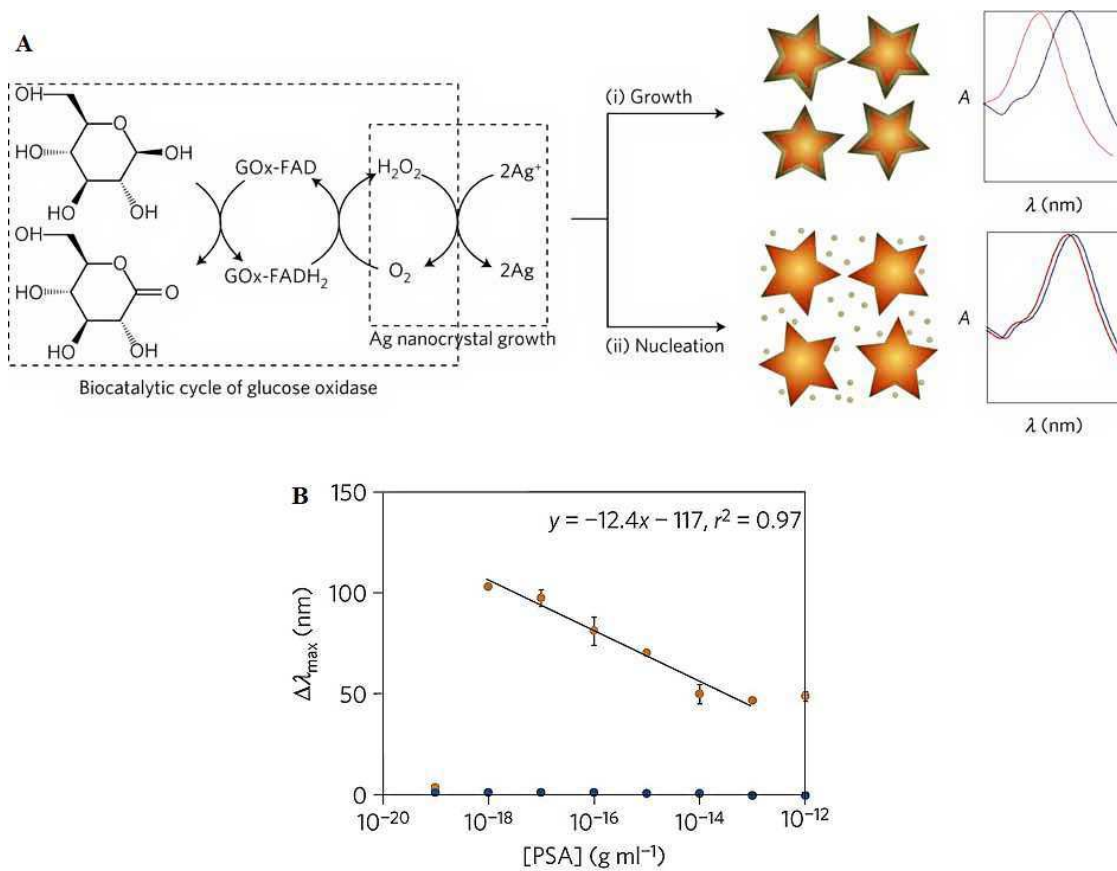
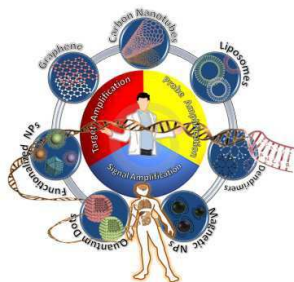


Fig. 11. (A) Schematic illustration of the proposed signal-generation mechanism by means of enzyme-guided crystal growth for the plasmonic ELISA assay. **(B)** Immunoassay for the ultrasensitive detection of PSA with GOx-labelled antibodies and of PSA (red) and BSA (green) spiked into whole serum. Reprinted with permission from ref. 87, copyright © 2012, Nature Publishing group.

Table of Content

A survey of the recent, significant developments on nanomaterials enabled ultrasensitive DNA and gene mutation assays is presented.



Analyst Accepted Manuscript